

อนุพันธ์ของคาร์บาโซลและทรุกซีนสำหรับไดโอดอินทรีย์เปล่งแสง

นายคุณุสรณ์ รักษาสรณ์

วิทยานิพนธ์นี้เป็นส่วนหนึ่งของการศึกษาตามหลักสูตรปริญญาวิทยาศาสตรมหาบัณฑิต
สาขาวิชาปิโตรเคมีและวิทยาศาสตร์พอลิเมอร์
คณะวิทยาศาสตร์จุฬาลงกรณ์มหาวิทยาลัย
ปีการศึกษา 2555

ลิขสิทธิ์ของจุฬาลงกรณ์มหาวิทยาลัย
บทคัดย่อและแฟ้มข้อมูลฉบับเต็มของวิทยานิพนธ์ตั้งแต่ปีการศึกษา 2554 ที่ให้บริการในคลังปัญญาจุฬาฯ (CUIR)
เป็นแฟ้มข้อมูลของนิสิตเจ้าของวิทยานิพนธ์ที่ส่งผ่านทางบัณฑิตวิทยาลัย

The abstract and full text of theses from the academic year 2011 in Chulalongkorn University Intellectual Repository (CUIR)
are the thesis authors' files submitted through the Graduate School.

DERIVATIVES OF CARBAZOLE AND TRUXENE FOR ORGANIC LIGHT-
EMITTING DIODES

Mr. DanusornRaksasorn

A Thesis Submitted in Partial Fulfillment of the Requirements
for the Degree of Master of Science Program in Petrochemistry and Polymer Science

Faculty of Science

Chulalongkorn University

Academic Year 2012

Copyright of Chulalongkorn University

Thesis Title DERIVATIVES OF CARBAZOLE AND TRUXENE FOR
 ORGANIC LIGHT-EMITTING DIODES

By Mr. DanusornRaksasorn

Field of Study Petrochemistry and Polymer Science

Thesis Advisor Assistant Professor PaitoonRashatasakhon, Ph.D.

Accepted by the Faculty of Science, Chulalongkorn University in
Partial Fulfillment of the Requirements for the Master's Degree

..... Dean of the Faculty of Science
(Professor SupotHannongbua, Dr.rer.nat)

THESIS COMMITTEE

.....Chairman
(Assistant Professor Warinthorn Chavasiri, Ph.D.)

.....Thesis Advisor
(Assistant Professor PaitoonRashatasakhon, Ph.D.)

.....Examiner
(Assistant Professor VarawutTangpasuthadol, Ph.D.)

.....External Examiner
(PannraphatTakolpuckdee, Ph.D.)

คุณสรณ์ รักษาสรณ์: อนุพันธ์ของคาร์บาโซลและทรุกซีนสำหรับไดโอดอินทรีย์เปล่งแสง.
(DERIVATIVES OF CARBAZOLE AND TRUXENE FOR ORGANIC LIGHT-
EMITTING DIODES) อ.ที่ปรึกษาวิทยานิพนธ์หลัก: ผศ.ดร. ไพฑูรย์ รัชตะสาคร, 63 หน้า.

ได้ออกแบบและสังเคราะห์อนุพันธ์ใหม่ของคาร์บาโซลและทรุกซีน 2 ชนิด เพื่อนำไปใช้เป็นวัสดุส่งผ่านประจุบวกในไดโอดอินทรีย์เปล่งแสงใช้ปฏิกิริยาอัลคิลเลชันของหมู่เมทิลีนในทรุกซีนในการสังเคราะห์เพื่อเพิ่มความสามารถในการละลายของสารในตัวทำละลายอินทรีย์และป้องกันการจับตัวของสารโดยการเกิดการซ้อนของพายออบิทัล สามารถสังเคราะห์สารเป้าหมายได้ในปริมาณผลิตภัณฑ์ระดับปานกลางด้วยปฏิกิริยาไอโอดีนชันของแกนกลางทรุกซีนและปฏิกิริยาควบคู่ระหว่างคาร์บอนและไนโตรเจนที่มีโลหะทองแดงเป็นตัวเร่งปฏิกิริยา ในสถานะสารละลายสารทั้งสองดูดกลืนแสงและคายพลังงานแสงในช่วงความยาวคลื่น 330-331 และ 367-391 นาโนเมตรตามลำดับ แต่ในสถานะฟิล์มบางความยาวคลื่นของการดูดกลืนแสงและการคายพลังงานแสงจะเปลี่ยนเป็น 315-333 และ 379-418 นาโนเมตร สารทั้งสองมีสมบัติทางความร้อนที่ดีเยี่ยมโดยมีค่าอุณหภูมิทรานซิชันแก้วสูงกว่า 240 องศาเซลเซียส เมื่อนำสารทั้งสองไปขึ้นรูปผนวกเป็นชั้นส่งผ่านประจุบวกในอุปกรณ์ไดโอดอินทรีย์เปล่งแสงที่มีอินเดียมทินออกไซด์เป็นแอนโนด มีลิเทียมฟลูออไรด์เคลือบบนแผ่นอะลูมิเนียมเป็นแคโทด และมีอะลูมิเนียมไตรไฮโดรควิโนลีนเป็นชั้นเปล่งแสง พบว่าอุปกรณ์ที่มีสาร 2 เป็นชั้นส่งผ่านประจุบวกจะให้ประสิทธิภาพที่ดีที่สุดโดยจะให้แสงสีเขียวจากชั้น Alq₃ ออกมาและมีค่าความสว่างสูงสุดที่ 9,658 แคนเดลาต่อตารางเมตร ที่ 9.2 โวลต์ โดยมีค่าศักย์ไฟฟ้าเริ่มต้น 3.6 โวลต์

สาขาวิชา ปิโตรเคมีและวิทยาศาสตร์พอลิเมอร์ลายมือชื่อนิสิต.....
ปีการศึกษา2555.....ลายมือชื่ออ.ที่ปรึกษาวิทยานิพนธ์หลัก.....

##5372249523: MAJORPETROCHEMISTRY AND POLYMER SCIENCE
 KEYWORDS: TRUXENE/ CARBAZOLE / ORGANIC LIGHT-EMITTING
 DIODES/ HOLE-TRANSPORTING

DANUSORN RAKSASORN:DERIVATIVES OF CARBAZOLE AND
 TRUXENE FOR ORGANIC LIGHT-EMITTING DIODES.ADVISOR:
 ASSIST. PROF. PAITON RASHATASAKHON, Ph.D., 63 pp.

Two new derivatives of carbazole and truxene (compound **1** and **2**) were redesigned and synthesized for application as hole-transporting material in Organic Light-Emitting Diodes (OLEDs). The synthesis involved the alkylation at the methylene groups in truxene in order to facilitate the solubility in organic solvent and prevent the aggregation of compound by pi-pi stacking. The iodination of truxene core and Cu-catalyzed C-N coupling with carbazole or 3,6-di(9-carbazolyl) carbazole then gave rise to the target compounds in moderate yields. In solution phase, the compounds displayed maximum absorption and emission wavelengths at 330-331 and 367-391 nm, respectively, while they showed absorption at 315-333 and emission at 379-418 nm as thin film state. Both compounds possess excellent thermal stabilities with high glass transition temperatures (T_g) of above 240 °C. These compounds were fabricated as hole-transporting materials in organic light-emitting devices. The device having the structure of ITO/PEDOT:PSS/2/Alq₃/LiF:Alexhibited bright green emission with a maximum luminescence of 9,658 cd/m² at 9.2 V and a turn-on voltage of 3.6 V.

Field of Study :Petrochemistry and Polymer
 Academic Year :2012.....

Student's Signature
 Advisor's Signature

ACKNOWLEDGEMENTS

First of all, I would like to express my sincere gratitude to my thesis advisor, Assistant Professor Paitoon Rashatasakhon, Ph.D. for valuable advice, guidance and kindness throughout this research. Sincere thanks are also extended to Assistant Professor Warinthorn Chavasiri, Ph.D., Assistant Professor Varawut Tangpasuthadol, Ph.D., and Pannraphat Takolpuckdee, Ph.D., attending as the committee members, for their valuable comments and suggestions.

I would like to especially thank Associate Professor Mongkol Sukwattanasinitt, Ph.D. for valuable guidance and Associate Professor Vinich Promarak, Ph.D. and Assistant Professor Taweesak Sudyoasuk, Ph.D., Ubon Ratchathani University for kind support on OLED work.

In particular, I am thankful to the Center for Petroleum, Petrochemicals, and Advanced Materials for supporting my thesis. Gratitude is also extended to the members of my research group for their helpful discussion.

Finally, I would like to specially thank my family and friends for their encouragement and understanding throughout. I would not be able to reach this success without them.

CONTENTS

	Page
ABSTRACT (THAI).....	iv
ABSTRACT (ENGLISH).....	v
ACKNOWLEDGEMENTS.....	vi
CONTENTS.....	vii
LIST OF TABLES.....	ix
LIST OF FIGURES.....	x
LIST OF ABBREVIATIONS.....	xv
CHAPTER I INTRODUCTION.....	1
1.1 Introduction to OLED.....	1
1.2 OLED structure and operation.....	3
1.3 Organic electroluminescent materials.....	4
1.4 Hole-transporting materials (HTMs).....	6
1.5 Emitting materials (EMMs)	6
1.6 OLED device fabrication technologies.....	7
1.7 Literature reviews.....	8
CHAPTER II EXPERIMENTAL.....	12
2.1 Synthesis.....	12
2.1.1 Instruments and Equipment.....	12
2.1.2 Synthetic procedures.....	13
2.2 OLED device fabrication section.....	18
2.2.1 Commercially available materials.....	18
2.2.2 Reagents.....	18
2.2.3 Instruments.....	19
2.2.4 Organic thin film preparation and characterization.....	20
2.2.5 Spin coating technique of the organic thin films.....	20
2.2.6 Device fabrication.....	22

	Page
2.2.7 Patterning process for ITO-coated glasses.....	23
2.2.8 Cleaning process for the patterned ITO glasses.....	23
2.2.9 Spin-coating method of PEDOT:PSS.....	24
2.2.10 Organic thin film deposition.....	25
2.2.11 Emissive layer deposition.....	25
2.2.12 Cathode deposition.....	25
2.2.13 Device measurement.....	26
CHAPTER III RESULTS AND DISCUSSION.....	29
3.1 Synthesis.....	29
3.2 Optical property.....	37
3.3 Electrochemical property	39
3.4 Thermal property.....	41
3.5 Hole transporting property.....	42
3.5.1 Investigation of hole transporting property.....	42
3.5.2 Investigation of thickness of hole transporting layer.....	45
CHAPTER IV CONCLUSION.....	47
REFERENCES.....	48
APPENDIX.....	56
VITAE.....	63

LIST OF TABLES

	Page
Table 2.1 Commercially available materials for OLED device fabrication..	18
Table 2.2 List of reagents.....	19
Table 3.1 C-N coupling conditions for compound 1	35
Table 3.2 Optical properties of compound 1 and 2 measured in CHCl ₃ solutions and thin films.....	39
Table 3.3 The electrochemical properties of compound 1 and 2	40
Table 3.4 The thermal properties of compound 1 and 2	42
Table 3.5 Electroluminescent properties of device 1-5.....	44
Table 3.6 Electroluminescent properties of device 6-9.....	46
Table 3.7 AFM image of compound 2 at 1, 2, 3 and 5 %w/v.....	46

LIST OF FIGURES

		Page
Figure 1.1	OLED display.....	1
Figure 1.2	Comparison of brightness and contrast between OLED and LCD display.....	2
Figure 1.3	Chemical structures of Alq ₃ and diamine.....	2
Figure 1.4	Schematic structure (top) and energy level diagram (bottom) of (a) single-layer OLED and (b) multi-layer OLED.....	4
Figure 1.5	Chemical structure of Poly(p-phenylenevinylene) (PPV).....	5
Figure 1.6	Chemical structures of NPB and TPD.....	6
Figure 1.7	Jablonski diagram.....	7
Figure 1.8	Chemical structures of DCM and PF derivative.....	7
Figure 1.9	Chemical structures of G1CBC and G2CBC.....	8
Figure 1.10	Chemical structures of compound 1-3.....	9
Figure 1.11	Chemical structures of G2CB and G2CC.....	10
Figure 1.12	Chemical structures of Tr-TPA3 and Tr-TPA9.....	10
Figure 2.1	Preparation and characterization of organic thin film.....	20
Figure 2.2	(a) A thermal evaporator which consists of (1) vacuum chamber, (2) high vacuum pump system; (i) backing pump, (ii) diffusion pump and (iii) cooler of diffusion pump, (3) volume control of evaporation source heater, (4) thickness monitor of quartz crystal oscillator, (5) vacuum gauge, and (6) vacuum gauge monitor and (b) vacuum chamber consisting of (1) evaporation source heaters (alumina filament bolts), (2) sensor of the quartz crystal oscillator, (3) source shutter, and (4) substrate holder.....	21
Figure 2.3	Fabrication of OLED.....	22
Figure 2.4	(a) ITO-coated glass, (b) ITO-coated glass covered with 2 x 10 mm of negative dry film photo resist and (c) patterned ITO glass.....	23

	Page
Figure 2.5 Spin-coating methods by using a spin coater. (a) PEDOT:PSS solution in the syringe, (b) nylon filter, and (c) fresh patterned ITO glass.....	24
Figure 2.6 Instrument for cathode deposition. (a) tungsten boats and (b) 2mm wide fingers of a shadow mask.....	26
Figure 2.7 OLED device.....	26
Figure 2.8 Instruments for determination of OLED device performance: (a) OLED test box, (b) lid of OLED test box, (c) calibrated photodiode, (d) multifunction optical meter, (e) digital sourcemeter, (f) USB spectrofluorometer, (g) probe of USB spectrofluorometer, (h) OLED device holder, (i) computer controller and recorder for digital source meter, multifunction optical meter, and USB spectrofluorometer	27
Figure 3.1 The synthesis of 8	29
Figure 3.2 ¹ H-NMR of 6 in CDCl ₃	30
Figure 3.3 ¹ H-NMR of 7 in CDCl ₃	30
Figure 3.4 ¹ H-NMR of 8 in CDCl ₃	31
Figure 3.5 The synthesis of tercarbazole dendron (5).....	32
Figure 3.6 ¹ H-NMR of 3 in DMSO- <i>d</i> ₆	32
Figure 3.7 ¹ H-NMR of 4 in CDCl ₃	33
Figure 3.8 ¹ H-NMR of 5 in CDCl ₃	33
Figure 3.9 The mechanism of Cu-catalyzed C-N coupling reaction.....	34
Figure 3.10 The synthesis of compound 1	35
Figure 3.11 ¹ H-NMR of compound 1 in CDCl ₃	36
Figure 3.12 The synthesis of compound 2	36
Figure 3.13 ¹ H-NMR of compound 2 in CDCl ₃	37
Figure 3.14 Normalized absorption spectra of compound 1 , 2 in CHCl ₃ and thin film.....	38
Figure 3.15 Normalized emission spectra of compound 1 , 2 in CHCl ₃ and thin film.....	39

	Page
Figure 3.16 The cyclic voltammograms of compound 1 and 2	40
Figure 3.17 Band diagram of ITO, compound 1 , compound 2 , Alq ₃ and LiF/Al.....	41
Figure 3.18 DSC curves of compound 1 and 2 at a heating rate of 10 °C/min under N ₂ atmosphere.....	42
Figure 3.19 Energy level diagram of device 1-5.....	43
Figure 3.20 Current density and luminance VS voltage characteristic of device 1-5.....	44
Figure 3.21 Device configuration of device 6-9.....	45
Figure 3.22 Current density and luminance VS voltage characteristic of device 6-9.....	45
Figure 1 ¹ H-NMR spectrum of 3,6-diiodo-9 <i>H</i> -carbazole(3).....	56
Figure 2 ¹ H-NMR spectrum of 9-acetyl-3,6-diiodo-carbazole(4).....	56
Figure 3 ¹ H-NMR spectrum of 3,6-di(9-carbazolyl) carbazole (5).....	57
Figure 4 ¹ H-NMR spectrum of truxene (6).....	57
Figure 5 ¹ H-NMR spectrum of 5,5,10,10,15,15-hexabutyl-truxene(7)...	58
Figure 6 ¹ H-NMR of 3 in DMSO- <i>d</i> ₆	58
Figure 7 ¹ H-NMR spectrum of compound 1	59
Figure 8 ¹³ C-NMR spectrum of compound 1	59
Figure 9 MALDI-TOF spectrum of compound 1	60
Figure 10 ¹ H-NMR spectrum of compound 2	60
Figure 11 ¹³ C-NMR spectrum of compound 2	61
Figure 12 MALDI-TOF spectrum of compound 2	61
Figure 13 TGA spectrum of compound 1	62
Figure 14 TGA spectrum of compound 2	62

LIST OF ABBREVIATIONS

A	Ampere
Å	Angstrom
Alq ₃	Tris(8-hydroxyquinoline)aluminium
Al	Aluminium
°C	Degree of celsius
cm ²	Square centimeter
Ca	Calcium
cd	Candela
CDCl ₃	Deuterated chloroform
CH ₂ Cl ₂	Methylene chloride
CRT	Cathode ray tube
Cu	Copper
CV	Cyclic voltammetry
d	Doublet
dd	Doublet of doublet
DMSO	Dimethyl sulfoxide
DMSO- <i>d</i> ₆	Deuterated dimethyl sulfoxide
DSC	Differential scanning calorimeter
EMMs	Emitting materials
EL	Electroluminescent
EML	Emitting layer
ETL	Electron-transporting layer
EtOAc	Ethyl acetate
eV	Electron volt
g	Gram (s)
h	Hour
HOMO	Highest occupied molecular orbital
HRMS	High resolution mass spectroscopy
H ₂ SO ₄	Sulfuric acid
HTL	Hole-transporting layer

HTMs	Hole-transporting materials
Hz	Hertz
ITO	Indium tin oxide
J	Coupling constant
K_2CO_3	Potassium carbonate
KI	Potassium iodide
KIO_3	Potassium iodate
LCD	Liquid crystal display
LED	Light-emitting diode
lm	Lumen
LiF	Lithium fluoride
LUMO	Lowest unoccupied molecular orbital
Mg	Magnesium
m^2	Square meter
m	Multiplet
mg	Milligram (s)
$MgSO_4$	Magnesium sulfate
min	Minute (s)
mL	Milliliter (s)
mmol	Millimole
M	Molar
MS	Mass spectroscopy
m.p.	Melting point
nm	Nanometer (s)
NMR	Nuclear magnetic resonance
NPB	4,4'-bis-[N-(1-naphthyl)-N-phenyl- amino]-biphenyl
OLED	Organic light-emitting diode
$Pd(PPh_3)_4$	Tetrakis(triphenylphosphine)palladium
ppm	Parts per million
PL	Photoluminescent
PEDOT:PSS	poly(3,4-ethylenedioxythiophene) poly(styrenesulfonate)
s	Singlet

t	Triplet
T_g	Glass transition temperature
TGA	Thermo gravimetric analysis
THF	Tetrahydrofuran
TLC	Thin layer chromatography
TPD	N,N'-diphenyl-N,N'-bis(3-methylphenyl)-1,1'-biphenyl-4,4'-diamine
V	Volt
W	Watt
%	Percent
δ	Chemical shift
ϵ	Molar absorptivity
λ	Wavelength
Φ	Fluorescence quantum yield

CHAPTER I INTRODUCTION

1.1 Introduction to OLED

Organic light emitting materials have been attracting attention of researchers from both industry and academic institutions which take place many technologies of display such as cathode ray tube (CRT), liquid crystal displays (LCD) and plasma displays due to their limitation, for examples, their bulky, low viewing angle, consuming more electrical power and color tunability. The bulky and heavy cathode ray tube displays (CRT) were replaced by LCD which flatter and slimmer than CRT. However, LCD has some disadvantages because they cannot emit light by itself and need background light source. The requirements of present display are good brightness, light quality, contrast, high resolution, improved color variation, low weight, reduction in thickness and cost, low power consumption. Therefore, OLED have been improved and developed to fulfill these requirements.



Figure 1.1 OLED displays [1]

OLED is the emission of light from fluorescence properties of organic material by electric power. They are attractive because OLEDs, working as displays, are flat and lighter in weight with emissive fast and operate at a very low voltage and offer the prospect of simple fabrication. They have excellent viewing angle and the potential of much low power consumption than backlit liquid crystal displays. From **Figure 1.2**,

OLED display shows better quality in brightness and contrast, which are important things to develop the next generation of flat panel displays over the LCD displays.

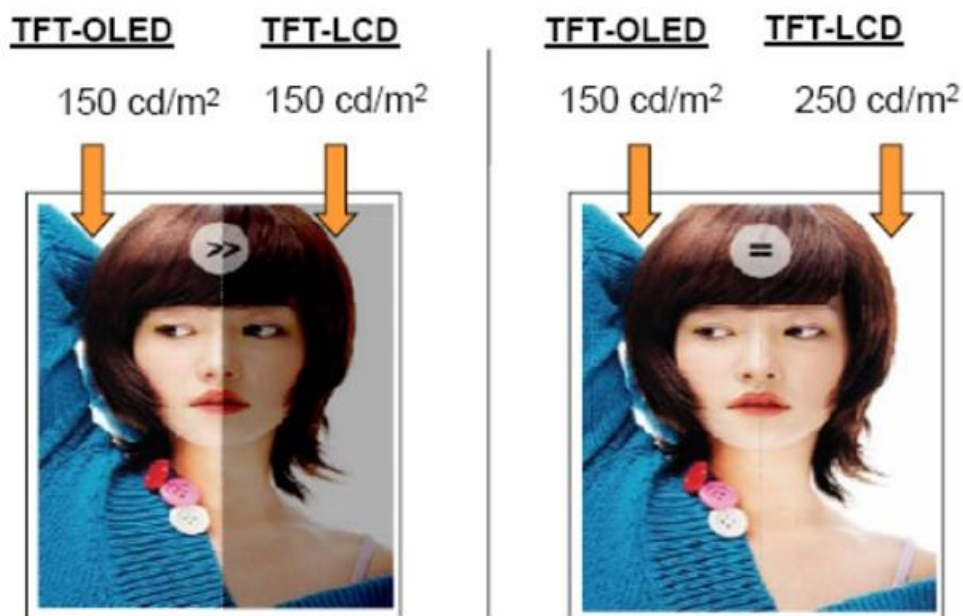
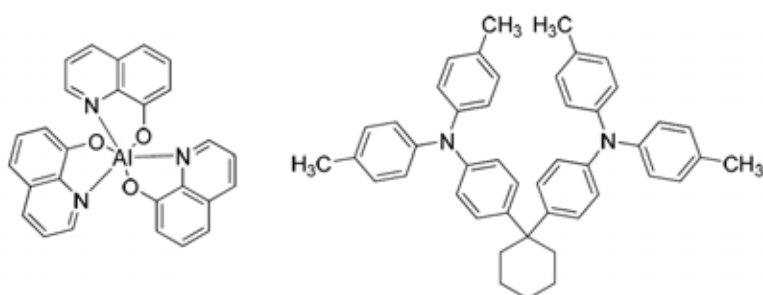


Figure 1.2 Comparison of brightness and contrast between OLED and LCD display [1]

In 1987, Ching W. Tang and Steven Van Slyke reported the first diode device at Eastman Kodak [2]. They developed a novel electroluminescent device with high brightness at low DC voltage. The device was fabricated by vapor deposition. The double layer of Alq₃ and diamine sandwiched between cathode and anode. The device showed high quantum efficiency, luminous efficiency, and brightness more than 100 cd/m² at driving voltage below 10 V.



Tris(8-hydroxyquinoline)
aluminium (Alq₃)

4,4'-(cyclohexane-1,1'-diyl)
bis(N,N-di-*p*-tolylaniline (Diamine)

Figure 1.3 Chemical structures of Alq₃ and diamine

1.2 OLED structure and operation [3-6]

The structure and operation of single-layer and multi-layer OLED are shown in **Figure 1.4**. The typical structure of OLED is the single-layer made from a single layer of organic film sandwiched between two electrodes, cathode and anode. The cathode electrode ejects electrons to the organic layer (emitting layer, EML). The cathode usually is a low work function metal alloy. The widely used materials are calcium (Ca) or magnesium (Mg). Aluminum (Al) is used to cover electrode to prevent an oxidation. In the anode, the converse applies, which supplied positively charged holes into the organic layer. A transparent electrode, indium tin oxide (ITO) is often used as anode material, so the light can emit through the device. The requirement of this electrode is low roughness with high work function.

The mechanism of OLED device starts from injection of electrons from the cathode into LUMO energy level of EML and holes from the anode into HOMO energy level of EML under applied voltage. Holes and electrons migrate through the EML and combined together, resulting in electronic excited state species called an exciton. The radiative decay of exciton results in emission of light. Thus, emission color can be determined by the energy gap of HOMO and LUMO of the emitting organic material. The brightness or intensity of the light depends on the applied electrical current.

Multi-layer OLED device is consisting of several layers that have different properties. The important factor to increase the performance of OLED device is to control the recombination of electrons and holes in the same amount by inserting hole-transporting or/and electron transporting layer between the electrodes to reduce the energy barrier between the electrodes and organic material layer for injection of charge to balance the amount of holes and electrons that inject into the emitting layer.

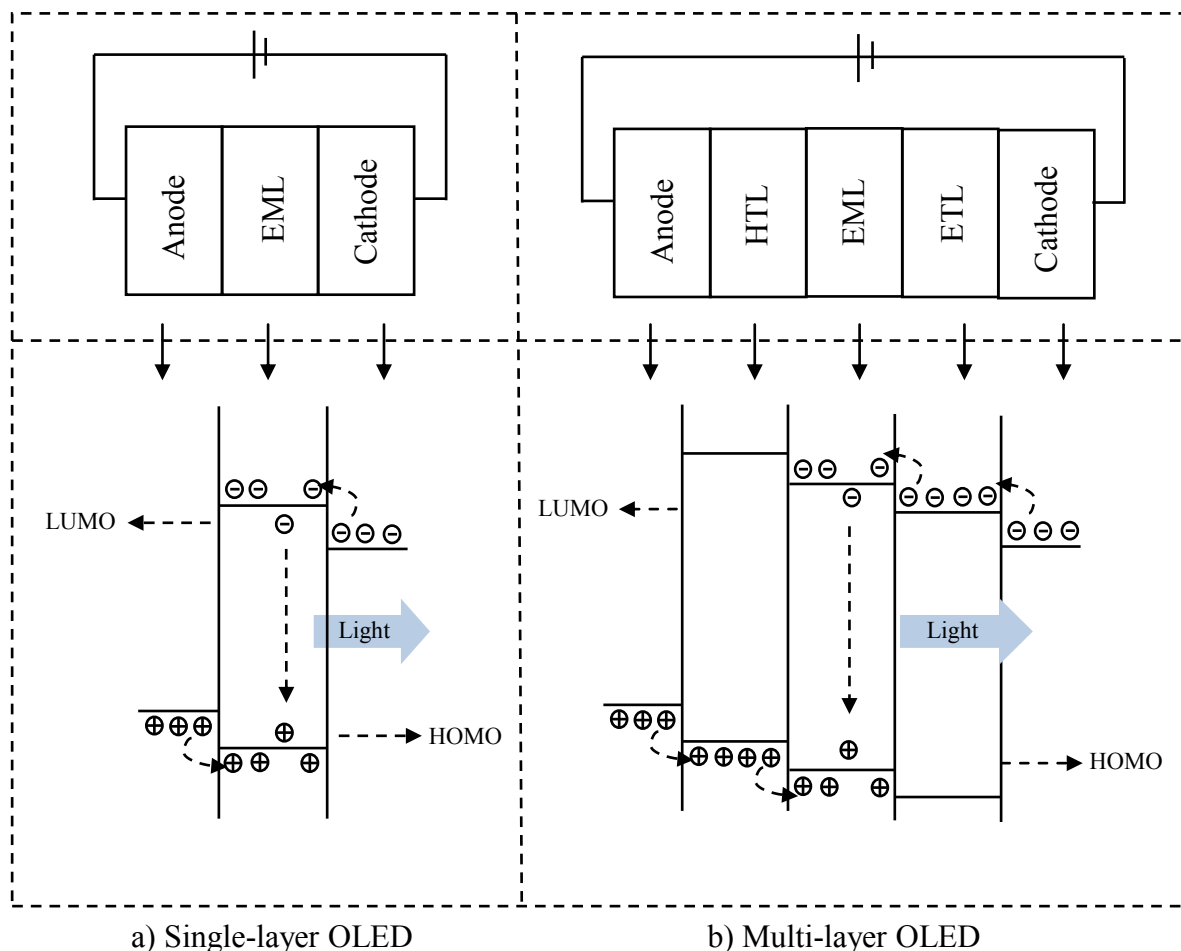


Figure 1.4 Schematic structure (top) and energy level diagram (bottom) of (a) Single layer OLED and (b) Multi-layer OLED.

1.3 Organic electroluminescent materials

Organic electroluminescent materials were mainly studied for the fabrication of practical OLED device. The primary reason is that the numerous organic materials with high fluorescence quantum efficiencies in the visible light. The development of organic electroluminescent materials has been separated into two classes; small molecules and polymer.

First, small molecules were firstly developed by Tang and Van Slyke whom improved the OLED efficiency and durability. The requirement for fabrication of highly stable OLED is the low molecular weight materials with specific optical and electronic properties, for example fluorescence, charge mobility, energy level, good film forming and high thermal stability [7-10]. Thermal stability is the one of the

significant factors for OLED device durability. Under thermal stress, most organic materials tend to turn into the thermodynamically stable crystalline state, which leads to device failure [11,12]. In general, high glass transition temperature (T_g) amorphous hole-transporting materials (AHTMs) are needed for highly efficient and long lifetime OLED devices [13-15]. Because they are in a thermodynamically non-equilibrium state and may exhibit glass transition phenomena usually associated with amorphous polymer. They may form transparent amorphous thin films, uniform by spin-coating method and thermal evaporation.

Second, the first polymer light emitting diode was reported by J.H. Burroughes and co-workers in 1990 [16-18]. Poly(p-phenylenevinylene) (PPV) film was prepared from solution-processable precursor polymer. The uniform, homogeneous and dense film was deposited on a pre-coated electrode substrate and deposited the top electrode on top of the PPV film. The device showed a threshold of charge injection below 14V. However, the quantum efficiency of the PPV devices was only 0.05%, much lower than the estimated photoluminescence (PL) quantum yield of about 8% for PPV. The main advantages of conjugated polymer are easy processing and mechanical flexibility. The polymer OLED requires small amount of power for production of light. For forming polymer thin film, vacuum deposition is not suitable method. However, polymer can be deposited by spin coating technique, the common method for deposited polymer thin film. This process is appropriate for large area film than thermal evaporation. However, the electrodes are needed to be deposited by thermal evaporation for fabrication of the multi-layer devices.

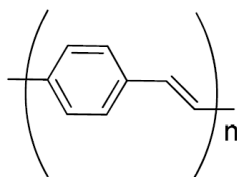


Figure 1.5 Chemical structure of Poly(p-phenylenevinylene) (PPV)

Therefore, the development of the performance of OLEDs is to design and synthesize materials with easy process, high thermal stability and charge transport properties. In this work, we design the new materials, which is the combination between the high thermal stability and hole transporting property of carbazole with

highly emissive truxene unit. The materials were synthesized and the OLED devices based on these materials were fabricated and investigated the performance of the devices.

1.4 Hole-transporting materials (HTMs)

The hole-transporting materials play a key role in transporting holes and prevent electrons get to the other side of the electrode without recombination with holes. The HTM should be stable in the radical cationic form and easily oxidized. The typical HTMs are 4,4'-bis-[N-(1-naphthyl)-N-phenyl- amino]-biphenyl (NPB)[19-22] and N,N'-diphenyl-N,N'-bis(3-methylphenyl)- 1,1'-biphenyl-4,4'-diamine (TPD) [23-28, 28a] which are widely used in OLED. The molecular structures are shown in **Figure 1.5**. They have an excellent hole transporting properties. However, they have low glass transition temperature (T_g) which affect the morphology at high operating temperature.

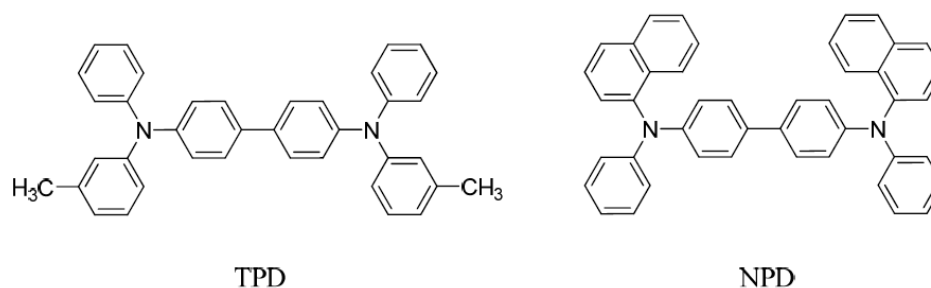


Figure 1.6 Chemical structures of NPB and TPD

1.5 Emitting materials (EMMs)

The emissive layer can be a material of organic fluorescence compounds or polymers with high efficiency, color purity and lifetime. The fluorescence principles are described by Jablonski diagram (**Figure 1.7**).

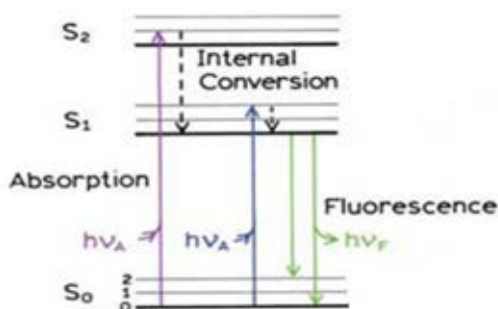


Figure 1.7 Jablonski diagram [29]

The requirements for full-color OLED display are consist of red, blue and green emitter to obtain a variety of colors by a combination of red, blue and green light. For example, the red emitter 4-(dicyanomethylene)-2- methyl-6-[4-(dimethylaminostyryl)-4H-pyran] (DCM) [30], a green emitter tris(8-hydroxyl-quinoline) aluminum (Alq₃) [31,32] and blue emitters NPD and polyfluorene (PF) derivatives (**Figure 1.8**) [33,34].

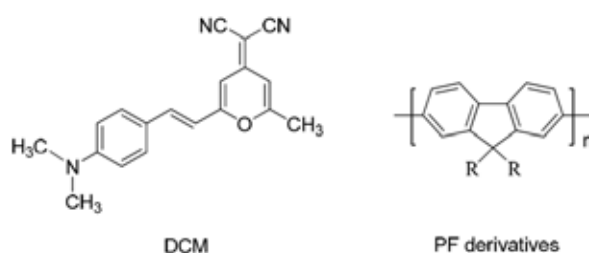


Figure 1.8 Chemical structures of DCM and PF derivatives

1.6 OLED devices fabrication technologies[35]

OLED devices can be fabricated in two ways, vacuum deposition technique and spin coating for solution technique. Vacuum deposition technique is the widely used technique of thin film deposition. The material is evaporated in vacuum. Then, the vacuum allows the vapor particles to go directly to the substrate and condense back to solid state. Therefore, this technique is suitable only for volatile and thermally stable materials. However, it takes more time to reach high vacuum state and is difficult to deposit over large area.

On the other hands, solution techniques offer several advantages over vacuum deposition such as easily fabrication procedure, large area coverage and low power

consumption. The simplest method for solution casting technique is using the centrifuge force by dropping small amount of the solution onto spinning head and spinning the solution, respectively. The centrifuge force will spread the solution into thin film layer on the top of substrate.

1.7 Literature reviews

This part will survey about application of carbazole and truxene derivatives as the HTMs for OLED.

In 2011, V. Promarak and coworkers [48] synthesized carbazole dendrimers, G1CBC and G2CBC (**Figure 1.9**) for using as holetransporting layer for OLED. G1CBC and G2CBC showed emission band in blue-purple region at 420 and 413 nm, respectively. G1CBC and G2CBC exhibited high glass transition temperature at 138 and 245 °C, respectively. To investigate the hole-transporting properties, the OLED with structures of ITO/HTL(50 nm)/Alq₃(50 nm)/LiF(0.5 nm):Al(200 nm) were fabricated. The device with G2CBC as an HTL shown maximum luminance is about 15,890 cd/m² at 13 V with a turn-on voltage of 3 V.

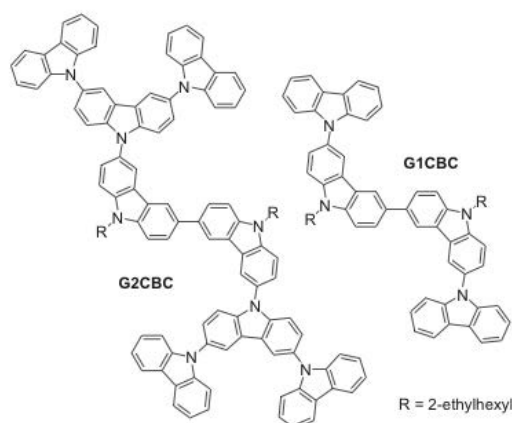


Figure 1.9 Chemical structures of G1CBC and G2CBC [48]

In 2010, T. Kumchoo and coworkers [49] successfully synthesized three derivatives of 3,6-dipyrenylcarbazole as blue light emitting and hole transporting materials. All compounds showed high glass transition temperatures above 160 °C. The devices with the structure of ITO/PEDOT:PSS/EML/LiF:Al having compound 1-3 as EML. The device with compound 3 exhibited the best performance with maximum luminance 1,600 cd/m² at 8.8 V and turn-on voltage of 3.8 V for blue

OLED. Then, The devices configurations of ITO/HTM/Alq₃/LiF/Al were fabricated using compound 1-3 as HTL and Alq₃ as EML. The device with compound 3 as HTL showed the maximum luminance of 9,300 cd/m² at 8.8 V with a turn-on voltage of 4.2 V for green OLED.

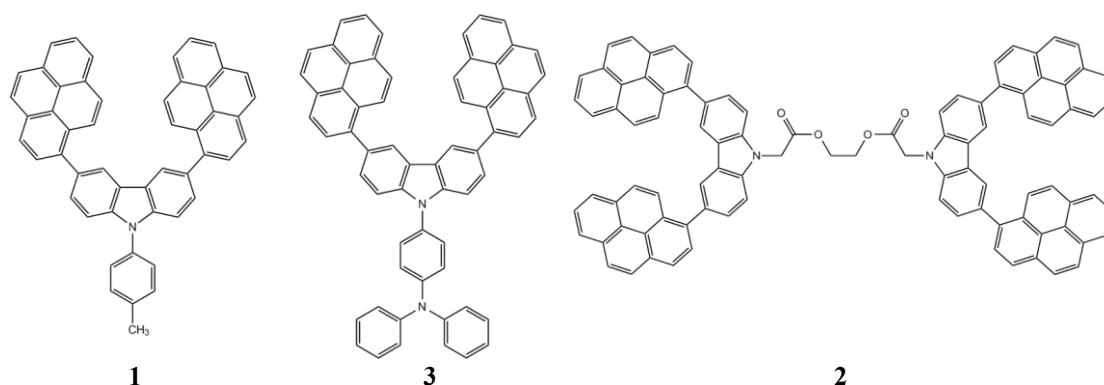


Figure 1.10 Chemical structures of compound 1-3 [49]

In 2008, V. Promarak and coworkers [50] synthesized a hole-transporting materials based on carbazole compounds (G2CB and G2CC) (**Figure 1.9**). G2CB and G2CC exhibited identical emission shapes in bluish-purple region with the maxima at 382 and 390 nm, respectively. G2CB and G2CC that containing carbazole moieties showed high T_g at 206 °C and 245 °C, respectively. The electrochemical properties of the G2CB and G2CC were investigated by cyclic voltammetry (CV) analysis. HOMO levels of G2CB and G2CC are 5.46 and 5.44 eV, respectively. LUMO levels of G2CB and G2CC were 2.18 and 2.23 eV, respectively. OLED devices with the structure of ITO/HTL(50 nm)/Alq₃(50 nm)/LiF(0.5 nm):Al(200 nm) were fabricated using compounds G2CB and G2CC as the HTL. The device with G2CC as an HTL has much better performance in terms of brightness, current and turn-on voltage than that with G2CB. In the case of ITO/G2CC/Alq₃/LiF:Al device, its maximum luminance is about 8900 cd/m² at 14 V with a turn-on voltage of 3.5 V. The ITO/G2CB/Alq₃/LiF:Al device shows the maximum luminance at 3000 cd/m² at 15 V with a turn-on voltage of 7.5 V.

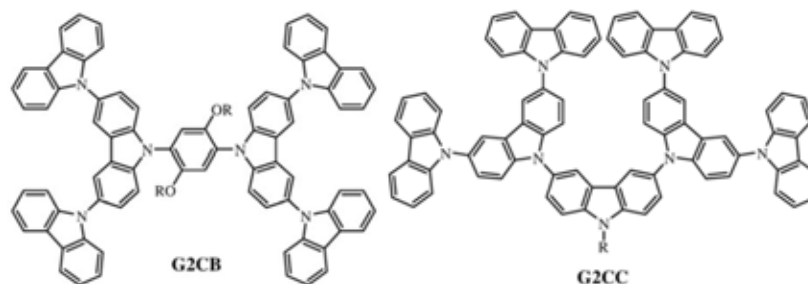


Figure 1.11 Chemical structures of G2CB and G2CC [50]

In 2009, Z. Yang and coworkers, [57] synthesized two solution-processable triphenylamine-based dendrimers with truxene core as hole-transporting materials for organic light-emitting diodes; Tr-TPA3 and Tr-TPA9 (**Figure 1.12**). The dendrimers showed excellent solubility in organic solvents, high thermal stability with high T_g above 110 °C and good film forming. Then, they fabricated devices which using these dendrimers as hole transporting layer and Alq_3 as emitting layer. The Tr-TPA9 based device exhibited the turn-on voltage of 2.5 V, the maximum luminance of about 11,058 cd/m^2 and the maximum current efficiency of 4.01 cd/A .

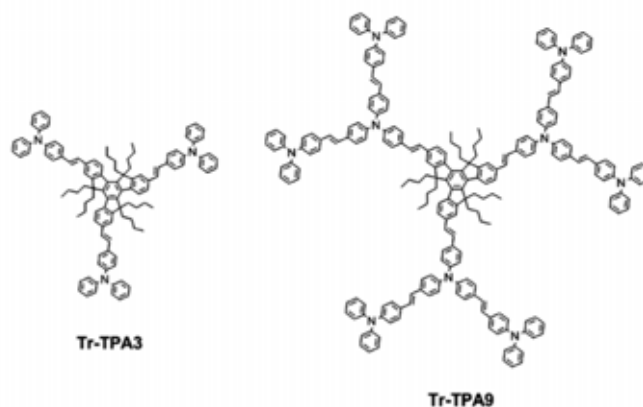


Figure 1.12 Chemical structures of Tr-TPA3 and Tr-TPA9 [57]

To improve the performance of OLED, the hole-transporting layer was inserted between the electrode and emissive layer. The commercial hole transporting material were NPB and TPD that have high hole transporting property, though, they have low glass transition temperature (T_g), which affect the morphology at high operating temperature. However, carbazole and truxene have been widely used as hole transporting materials due to their advantages, according to above literature reviews.

For carbazole derivatives, they have been extensively studied due to their optical and electrical properties [36-47]. The carbazole has strong absorption in the near UV region, donating ability of lone pair electron on nitrogen atom in carbazole ring, can be easily functionalized at its 3-, 6-, and 9- position and undergo reversible process which make them suitable as hole carriers. Therefore, they have been widely used as a hole transporting material in OLED devices.

For truxene derivatives [51-56], they have been an attractive building block for OLEDs, liquid crystals, fluorescent sensors, organic solar cells, and dendritic macromolecules due to their rigidity and highly emissive property. They can be easily functionalized at positions 2-, 7-, 12- and 5-, 10-, 15-.

On the other hand, there are no reports that incorporate carbazole and truxene into the same molecules. Therefore, in our current study, we incorporated highly emissive truxene unit with carbazole fragments with an aim to achieve new OLED materials with high hole transporting property and high thermal stability.

In summary, the objectives of this work are following:

- (1) To synthesize derivatives of carbazole and truxene as hole-transporting materials for OLED.
- (2) To characterize and study the electronic, photophysical, electrochemical and thermal properties of the target molecules.
- (3) To investigate their potential application as hole-transporting materials for OLED.

CHAPTER II EXPERIMENTAL

2.1 Synthesis

2.1.1 Instruments and Equipment

Thin layer chromatography (TLC) was performed on aluminium sheets precoated with silica gel (Merck Kieselgel 60 F₂₅₄) (Merck KGaA, Darmstadt, Germany). Column chromatography was performed on silica gel (Merck Kieselgel 60G) (Merck KGaA, Darmstadt, Germany). All ¹H-NMR spectra were recorded on Varian Mercury 400 MHz NMR spectrometer (Varian, USA) using CDCl₃ and DMSO-*d*₆. ¹³C-NMR spectra were recorded at 100 MHz on Bruker 400 MHz NMR spectrometer using the same solvent. Mass spectrawere recorded on a Microflex MALDI-TOF mass spectrometer (BrukerDaltonics) using doublyrecrystallized α-cyano-4-hydroxy cinnamic acid (CCA) as a matrix. Absorption spectra were measured by a ShimadzuUV-2550 UV-Vis spectrophotometer. Fluorescence spectra were obtained from an Agilent technologies Cary Eclipsespectrofluorometer.

The fluorescence quantum yields (Φ) were determined by comparison with a standard of known fluorescence quantum yield according to the following equation [58,59].

$$\Phi_{X=} \Phi_{ST} \left(\frac{Slope_X}{Slope_{ST}} \right) \left(\frac{\eta_X^2}{\eta_{ST}^2} \right)$$

Where the subscripts X refer to the unknown samples and ST refers to the standard 2-aminopyridine solution in 0.01 M H₂SO₄, whose fluorescence quantum yield is known to be 0.60, Φ is the fluorescence quantum yield, *Slope* is the slope from the plot of integrated fluorescence intensity versus absorbance, and η is the refractive index of the solvent. The refractive indexes of CHCl₃ and 0.01 M H₂SO₄ were 1.445 and 1.333, respectively.

The electrochemical analysis by cyclic voltametry was performed using an AUTOLAB spectrometer. All measurements were made at room temperature on sample solutions in freshly distilled dichloromethane with 0.1 M tetra-n-butylammoniumhexafluorophosphate as electrolyte. Dichloromethane was distilled

from calcium hydride and the electrolyte solutions were degassed by nitrogen bubbling. A glassy carbon working electrode, a platinum wire counter electrode, and a Ag/AgNO₃ (Sat.) reference electrode were used in all cyclic voltammetry experiments.

Thermal experiments with Differential Scanning Calorimeter (DSC) were performed on Mettler Toledo DSC 822^e and Thermogravimetric Analysis (TGA) were studied using Simultaneous Thermal Analyzer Netzsch 409. Melting point were measured on scientific melting point (Bibby)

2.1.2 Synthetic procedures

3,6-diiodo-9H-carbazole(3)

A solution of carbazole (5.0 g, 30.14mmol) in acetic acid (50 mL) was added potassium iodide (6.8 g, 40.95mmol). Then, potassium iodate (9.8 g, 45.78mmol) was added. The reaction mixture was refluxed for 20 min. The reaction was allowed to cool to room temperature and diluted with EtOAc (50 mL) and water (50 mL). The aqueous layer was separated and extracted with EtOAc (2 × 50 mL). The combined organic layer was dried over MgSO₄, filtered, and concentrated under reduced pressure to give a brown solid residue. The crude product was purified by crystallization from acetone and hexane to yield **3** as light brown crystals. (12.6 g, 99.6%). ¹H NMR (DMSO-*d*₆): δ 11.55 (s, 1H), 8.57 (s, 2H), 7.66 (d, *J* = 10.2 Hz, 2H), 7.35 (d, *J* = 8.5 Hz, 2H). This data is consistent with those reported in the literature [49,61].

9-acetyl-3,6-diiodocarbazole (4)

A mixture of **3** (2.3 g, 5.51 mmol) was dissolved in acetic anhydride (21 mL) and added boron trifluoride diethyl etherate (0.1 mL) then refluxing for 20 min to yield **4** as white powder (2.3 g, 92%) ¹H NMR (CDCl₃): δ 8.25 (s, 1H), 7.96 (d, *J* = 8.8 Hz, 1H), 7.76 (d, *J* = 8.8 Hz, 1H), 2.84 (s, 2H). This data is consistent with those reported in the literature [61].

3,6-di(9-carbazolyl) carbazole(5)

A mixture of carbazole (6.2 g, 37.12 mmol), **4** (7.8 g, 17.04 mmol) and copper(I) oxide (8.0 g, 55.68 mmol) in *N,N*-dimethylacetamide (DMAc) (150 mL) was heated to 160 °C for 36 h. The reaction mixture was cooled to room temperature and then filtered through Celite. The filtrate was poured into methanol (2 L). The mixture of acetylated carbazole trimer was obtained by filtration. Then, the mixture (3.6 g) was dissolved in THF (175 mL), DMSO (75 mL), H₂O (5 mL) and KOH (3.0 g, 69.09 mmol) was added and refluxed for 2 h. The reaction mixture was cooled to room temperature, neutralized by HCl, and then poured into water to give final mixture. The carbazole trimer was isolated by silica gel column chromatography using 4:1 hexane/ethyl acetate with 2% Et₃N as the eluent to yield (57% two steps) ¹H NMR (CDCl₃): δ 8.48 (s, 1H), 8.20 (s, 2H), 8.17 (d, *J* = 7.7 Hz, 4H), 7.70 (d, *J* = 8.6 Hz, 2H), 7.62 (dd, *J* = 8.6, 1.8 Hz, 2H), 7.44 – 7.34 (m, 8H), 7.33 – 7.24 (m, 6H). This data is consistent with those reported in the literature [61].

10,15-dihydro-5H-diindeno[1,2-a:1',2'-c]fluorene (Truxene) (6)

A mixture of 3-phenylpropionic acid (10.0 g, 66.72 mmol) and Polyphosphoric acid (50 g) was heated at 60 °C for 60 min under nitrogen atmosphere. Water (5 mL) was then added to the reaction and temperature was raised to 160 °C for 3 h. After the reaction was cooled to room temperature, the mixture was poured into ice water and gray powder was filtered and washed with water. The crude product was purified by recrystallization from toluene to yield **6** as light-yellow solid (49%). ¹H NMR (CDCl₃): δ 7.92 (d, *J* = 7.5 Hz, 1H), 7.68 (d, *J* = 7.3 Hz, 1H), 7.50 (t, *J* = 7.2 Hz, 1H), 7.39 (t, *J* = 7.2 Hz, 1H), 4.22 (s, 2H). This data is consistent with those reported in the literature [62].

5,5,10,10,15,15-hexabutyl-truxene (7)

A solution of truxene (**6**) (1.0 g, 2.92 mmol) in DMF (50 mL) at 0 °C under nitrogen, NaH (1.2 g, 29.80 mmol) was added and the solution was allowed to warm to room temperature and stirred for 30 min, then *n*-butyl bromide (3.2 mL) was added for 24 h. The mixture was poured into water and extracted with EtOAc. The combined organic layer was dried over MgSO₄, filtered, and concentrated under

reduce pressure. The crude product was purified by silica gel column chromatography using hexane as the eluent to yield **7** as white solid (1.5 g, 75%). ^1H NMR (CDCl_3): δ 8.38 (d, $J = 7.4$ Hz, 1H), 7.47 (d, $J = 5.9$ Hz, 1H), 7.43 – 7.31 (m, 2H), 3.09 – 2.88 (m, 2H), 2.20 – 2.00 (m, 2H), 1.02 – 0.79 (m, 4H), 0.61 – 0.35 (m, 10H).

5,5,10,10,15,15-hexabutyl-2,7,12-triiodo-truxene(8)

A solution of **7** (0.5 g, 0.74 mmol) in 5 ml of solvent mixture ($\text{CH}_3\text{COOH}:\text{H}_2\text{SO}_4:\text{H}_2\text{O} = 100:40:3$) and added 1 mL of CCl_4 . After adding KIO_3 (0.2 g, 0.75 mmol) and I_2 (0.9 g, 3.72 mmol), the mixture was heated to 80°C and stirred for 3 h. The reaction was cooled to room temperature and poured into water. The crude product was obtained by filtration and purified by recrystallization from ethanol to afford white powder of **8** (0.7 g, 84%). ^1H NMR (CDCl_3): δ 8.07 (d, $J = 8.4$ Hz, 1H), 7.76 (s, 1H), 7.71 (d, $J = 8.4$ Hz, 1H), 2.91 – 2.77 (m, 2H), 2.08 – 1.95 (m, 2H), 0.99 – 0.78 (m, 4H), 0.59 – 0.30 (m, 10H). This data is consistent with those reported in the literature [62]

Compound 1

A mixture of **8** (0.1 g, 0.10 mmol), carbazole (0.1 g, 0.73 mmol), Cu bronze powder (0.2 g, 2.69 mmol) and K_2CO_3 (0.2 g, 1.53 mmol) in degassed nitrobenzene (1 mL) was refluxed for 48 h under N_2 atmosphere. The resulting brown solution was allowed to cool to room temperature and extracted with CH_2Cl_2 (3×50 mL). The combined organic layer was dried over MgSO_4 , filtered, and concentrated under reduce pressure. The crude product was purified by silica gel column chromatography using 4:1 hexane/ CH_2Cl_2 as the eluent to yield (0.05 g, 41%). ^1H NMR (CDCl_3): δ 8.60 (d, $J = 8.5$ Hz, 1H), 8.22 (d, $J = 7.8$ Hz, 2H), 7.73 (s, 1H), 7.66 (d, $J = 8.3$ Hz, 1H), 7.59 (d, $J = 8.2$ Hz, 2H), 7.49 (t, $J = 7.2$ Hz, 2H), 7.35 (t, $J = 7.2$ Hz, 2H), 3.15 – 3.02 (m, 2H), 2.27 – 2.15 (m, 2H), 1.13 – 1.01 (m, 4H), 0.77 (dt, $J = 23.8, 12.5$ Hz, 4H), 0.62 (t, $J = 7.3$ Hz, 6H). ^{13}C NMR (CDCl_3): δ 155.5, 145.6, 140.9, 139.1, 138.1, 136.2, 125.95, 125.77, 124.7, 123.5, 120.8, 120.4, 120.0, 109.9, 56.0, 36.6, 26.7, 22.9, 13.9 ppm. MALDI-TOF-MS: found 1173.768 ($[\text{M}]^+$ calcd: 1173.69)

Compound 2

A mixture of **8** (0.1 g, 0.10mmol), **5**(0.2 g, 0.37 mmol), Cu bronze powder (0.1 g, 2.05mmol) and K₂CO₃ (0.2 g, 1.56mmol) in degassed nitrobenzene (1 mL) was refluxed for 48 h under N₂ atmosphere. The resulting brown solution was allowed to cool to room temperature and extracted with CH₂Cl₂ (3 × 50 mL). The combined organic layer was dried over MgSO₄, filtered, and concentrated under reduce pressure. The crude product was purified by silica gel column chromatography using 4:1 hexane/CH₂Cl₂ as the eluent to yield (0.1 g, 50%). ¹H NMR (CDCl₃): δ 8.80 (d, *J* = 8.5 Hz, 1H), 8.40 (s, 2H), 8.22 (d, *J* = 7.5 Hz, 4H), 7.99 (s, 1H), 7.96 – 7.85 (m, 3H), 7.75 (d, *J* = 8.7 Hz, 2H), 7.48 (q, *J* = 8.3 Hz, 8H), 7.34 (t, *J* = 7.1 Hz, 4H), 3.33 – 3.20 (m, 2H), 2.48 – 2.36 (m, 2H), 1.27 – 1.10 (m, 4H), 1.03 – 0.80 (m, 5H), 0.72 (t, *J* = 7.3 Hz, 6H). ¹³C NMR (100 MHz, CDCl₃): δ 156.2, 146.2, 142.0, 140.9, 139.9, 138.4, 136.0, 130.8, 126.6, 126.3, 126.1, 125.2, 124.4, 123.4, 121.2, 120.5, 120.1, 119.9, 111.5, 109.9, 56.5, 37.0, 27.0, 23.1, 14.2 ppm. MALDI-TOF-MS: found 2165.802 ([M]⁺ calcd: 2164.04)

2.2 OLED device fabrication section

2.2.1 Commercially available materials

The commercial sources and purities of materials used in these experiments are shown in **Table 2.1**. All materials were analytical grade and used without further purification, unless indicated.

Table 2.1 Commercially available materials for OLED device fabrication.

Materials	Purity (%)	Company
1" × 1" Indium oxide doped tin oxide (99.3 wt% In ₂ O ₃ :0.7wt% SnO ₂)-coated glasses (5-15 ohm/sq)	99.5	Kintec
Poly(3,4-ethylenedioxythiophene)–poly(styrene) (0.5 wt% PEDOT: 0.5 wt% PSS)	1.3	Baytron
Tris(8-hydroxyl-quinoline) aluminum (Alq ₃)	98	Sigma-Aldrich
Lithium fluoride (LiF)	99.98	ACROS
Aluminium (Al) wire	99.97	BDH
2,9-dimethyl-4,7-diphenyl-1,10-phenanthroline (BCP)	99.99	Sigma-Aldrich
N,N-diphenyl-N,N'-bis(1-naphthyl)-(1,1'-biphenyl)-4,4'-diamine (NPB)	99	Sigma-Aldrich
	99	Sigma-Aldrich

2.2.2 Reagents

The reagents were obtained from various suppliers as shown in **Table 2.2**. All reagents were analytical grade and used without further purification, unless indicated.

Table 2.2 List of reagents.

Reagents	Purity (%)	Company
Hydrochloric acid (HCl) 37%	36.5	Carlo Erba
Nitric acid (HNO ₃) 69%	68.5-69.5	BDH
Sodium hydroxide (NaOH)	99.99	Carlo Erba
Acetone	99.5	BDH

2.2.3 Instruments

The following instruments were used in this study:

- (1) Photoluminescence (PL) spectrophotometer (Perkin–Elmer, Model LS 50B)
- (2) Spin-coater (Chemat Technology, Model KW-4A)
- (3) Thermal evaporator (ANS Technology, Model ES280)
- (4) Digital source meter (Keithley, Model 2400)
- (5) Multifunction optical meter (Newport, Model 1835-C)
- (6) Calibrated photodiode (Newport, Model 818 UVCM)
- (7) USB Spectrofluorometer (Ocean Optics, Model USB4000FL)

2.2.4 Organic thin film preparation and characterization

The preparation process of organic thin films is described in **Figure 2.1**.

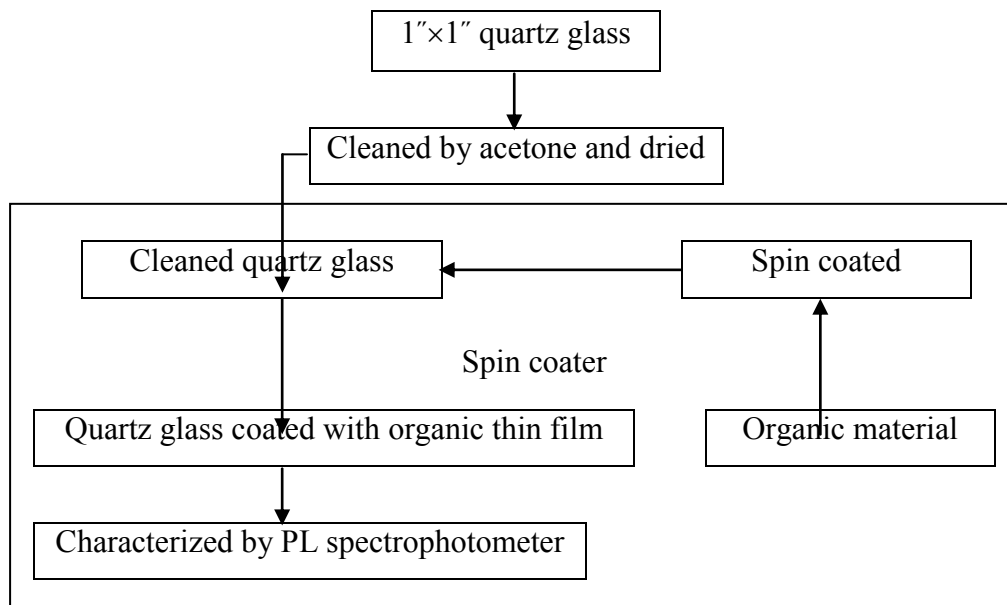
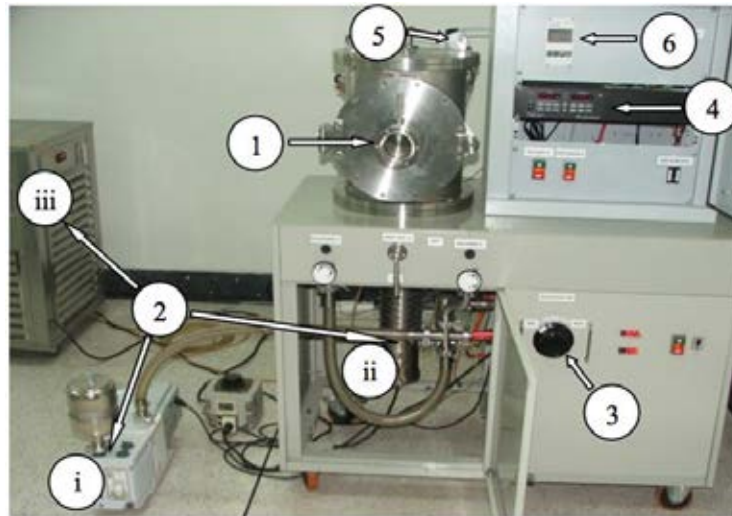


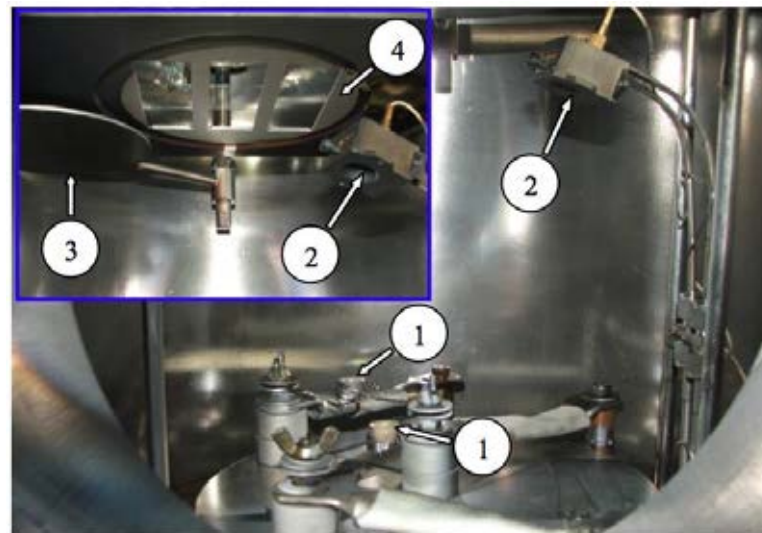
Figure 2.1 Preparation and characterization of organic thin film.

2.2.5 Spin coating technique of organic thin film

In order to study the photophysical properties of solid-state materials, organic thin films coating on quartz glass substrates (1" ×1") were prepared by spin coater. Prior to film deposition, the substrates were cleaned with acetone in ultrasonic bath followed by drying on a hotplate. The organic material was dissolved in the solution of THF:toluene (1:1 %v/v) and then filtered through a 0.45 μm pore size nylon filter (Orange scientific) and spin-coated onto a cleaned quartz glass surface at 2500 rpm for 30 sec. Finally, the quartz glass coated with the organic film was baked at 100 °C for 10 min.



(a)



(b)

Figure 2.2 (a) A thermal evaporator which consists of (1) vacuum chamber, (2) high vacuum pump system; (i) backing pump, (ii) diffusion pump and (iii) cooler of diffusion pump, (3) volume control of evaporation source heater, (4) thickness monitor of quartz crystal oscillator, (5) vacuum gauge, and (6) vacuum gauge monitor and (b) vacuum chamber consisting of (1) evaporation source heaters (alumina filament bolts), (2) sensor of the quartz crystal oscillator, (3) source shutter, and (4) substrate holder.

2.2.6 OLED device fabrication

The OLEDs fabrication process is described in **Figure 2.3**

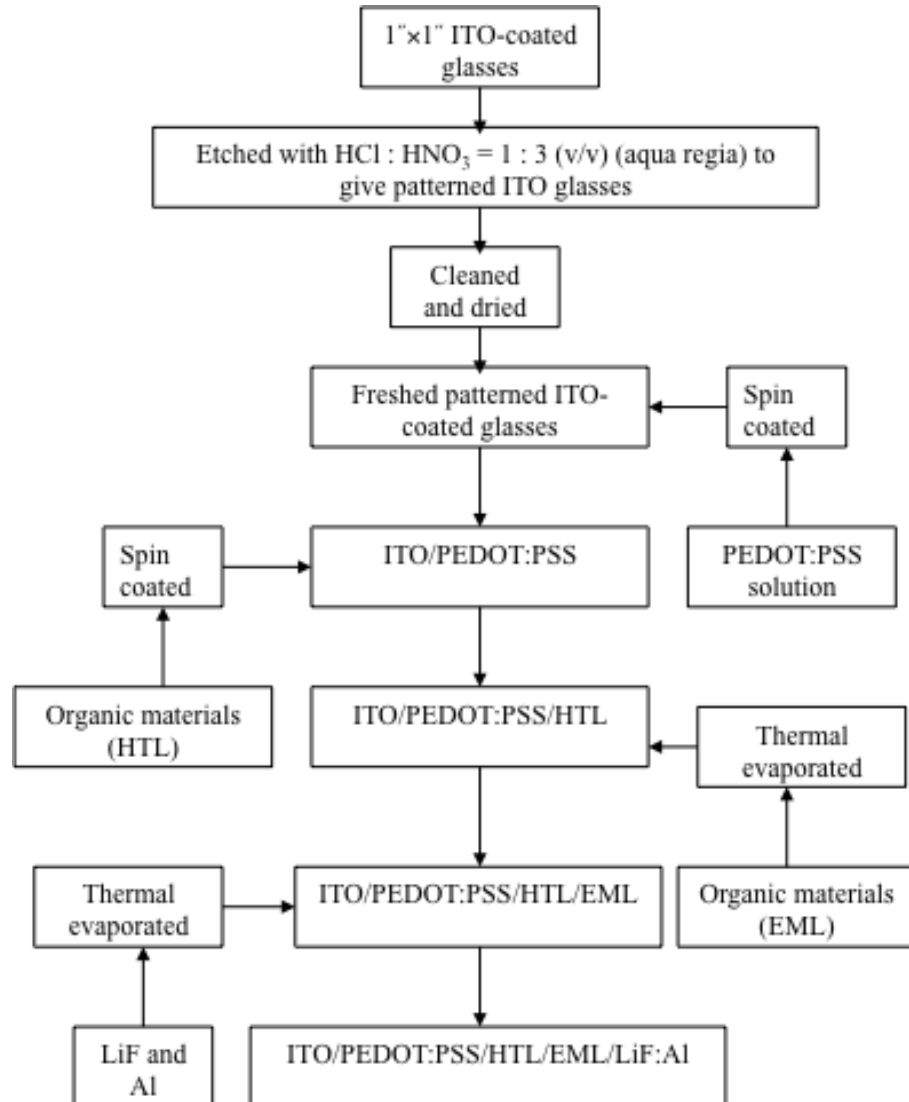


Figure 2.3 Fabrication of OLED.

2.2.7 Patterning process for ITO-coated glasses

The ITO-coated glasses (**Figure 2.4a**) were firstly etched to give a pattern of ITO sheet on glass. Prior to the patterning process, the ITO sheet on glass was covered with a 2 x 10 mm of negative dry film photo resist (Warf) [60]. The covered ITO glass (**Figure 2.4b**) was immersed in the solution of HCl:HNO₃ (1:3 v/v) (aqua regia) for 10 min, with stirring during the etching process. The etched ITO glass was cleaned by thoroughly rinsing with water and subsequently soaking in 0.5 M NaOH for 10 min to remove the negative dry film from an ITO-coated glass surface. Finally, these substrates were thoroughly rinsed with water to give the patterned ITO glasses as shown in **Figure 2.4c**.

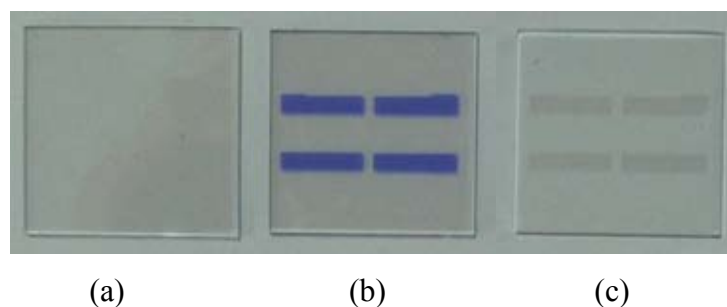


Figure 2.4 (a) ITO-coated glass, (b) ITO-coated glass covered with 2 x 10 mm of negative dry film photo resist and (c) patterned ITO glass.

2.2.8 Cleaning process for the patterned ITO glasses

The cleanliness of the ITO surface was an important factor in the performance of the OLEDs devices. The patterned ITO glasses were cleaned for 10 min with detergent in ultrasonic bath followed by a thorough rinse with de-ionized (DI) water and then subsequently ultra-sonicated in acetone for 10 min. Finally, the substrates were dried in vacuum oven at 100 °C to give fresh patterned ITO glasses.

2.2.9 Spin-coating method of PEDOT:PSS

A PEDOT:PSS solution was diluted with de-ionized (DI) water and stirred for 1 day. The spin-coating method was performed on a spin coater as shown in **Figure 2.5**. The diluted PEDOT:PSS solution was filtered through a 0.45 μm pore size nylon filter (Orange scientific) and spin-coated onto a fresh patterned ITO glass

surface at 2500 rpm for 30 sec. Finally, the patterned ITO glass coated with the PEDOT:PSS film was baked at 120 °C for 15 min for curing.

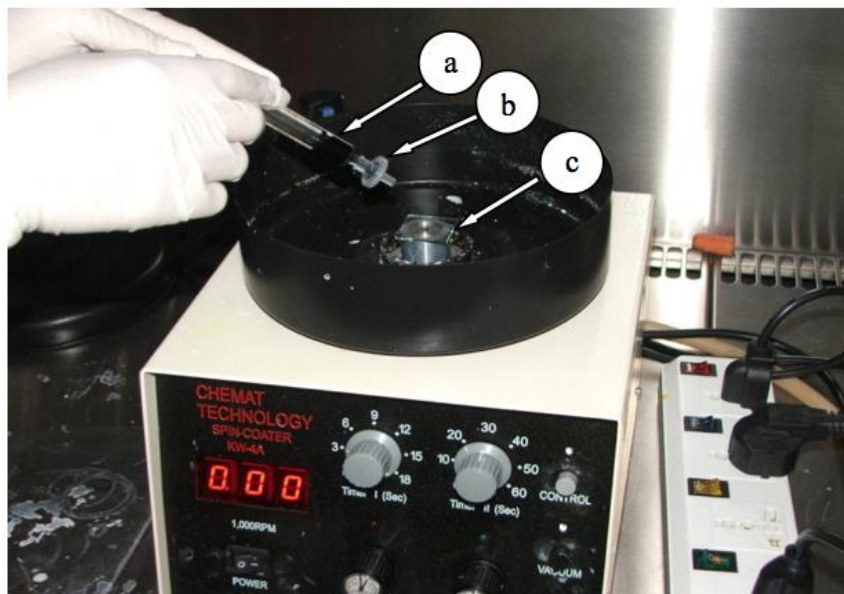


Figure 2.5 Spin-coating method by using a spin coater. (a) PEDOT:PSS solution in the syringe, (b) nylon filter, and (c) fresh patterned ITO glass.

2.2.10 Organic thin film deposition

The deposition of other organic layers was the next step in the fabrication of OLEDs. The organic layers were deposited using spin coating method (**Figure 2.2**) with the same procedure described in section 2.2.4. Prior to the deposition, the patterned ITO glass coated with PEDOT:PSS film or/and the fresh patterned ITO glass were placed on a substrate holder. The organic material was dissolved in the solution of THF:toluene (1:1 %v/v) and then filtered through a 0.45 μm pore size nylon filter (Orange scientific) and spin-coated onto a patterned ITO glass coated with PEDOT:PSS film or/and the fresh patterned ITO glass surface at 2500 rpm for 30 sec. Finally, the ITO glass coated with the organic film was baked at 100 °C for 10 min.

2.2.11 Emissive layer deposition

The organic layers were deposited using thermal evaporation. Prior to the deposition, the patterned ITO glasses coated with organic film were placed on a

substrate holder. The organic materials, such as Alq₃, were loaded in co-evaporation sources, alumina filament boat 1 and 2, respectively, into a vacuum chamber of the thermal evaporator. These organic materials were deposited on top of glass substrates by co-evaporation of the two source materials at a background pressure of approximately 1×10^{-5} mbar with 0.2 – 0.4 Å/sec evaporation rate.

2.2.12 Cathode deposition

Finally, an ultra thin LiF layer and Al cathode contact were sequentially co-evaporated from two tungsten boats through a shadow mask (**Figure 2.6**) with 2 mm wide slits arranged perpendicularly to the ITO fingers, to obtain the OLED with an active area of 2×2 mm² (**Figure 2.7**). The operating vacuum for evaporation of this cathode was under 1×10^{-5} mbar at high evaporation rates of 5 – 10 Å/sec. The thickness of LiF and Al of all devices were 0.5 and 150 nm, respectively.



Figure 2.6 Instrument for cathode deposition. (a) tungsten boats and (b) 2 mm wide fingers of a shadow mask.

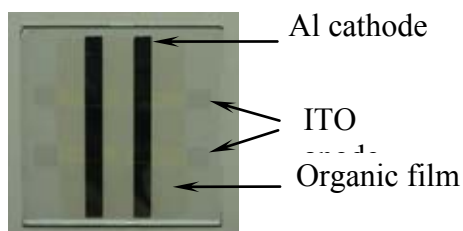


Figure 2.7 OLED device with 4 pixels. A pixel active area of a device is 2×2 mm².

2.2.13 Device measurement

The instruments for OLED device measurements are shown in **Figure 2.8**. The computer was used for controlling of the digital source meter, the multifunction optical meter, and the USB spectrofluorometer as well as recording the data. The digital source meter applied the voltages to the device and measured the resulting currents. The multifunction optical meter connected with the calibrated photodiode served in the measurement of the luminance (brightness). The USB spectrofluorometer was used for the EL spectra acquisition.

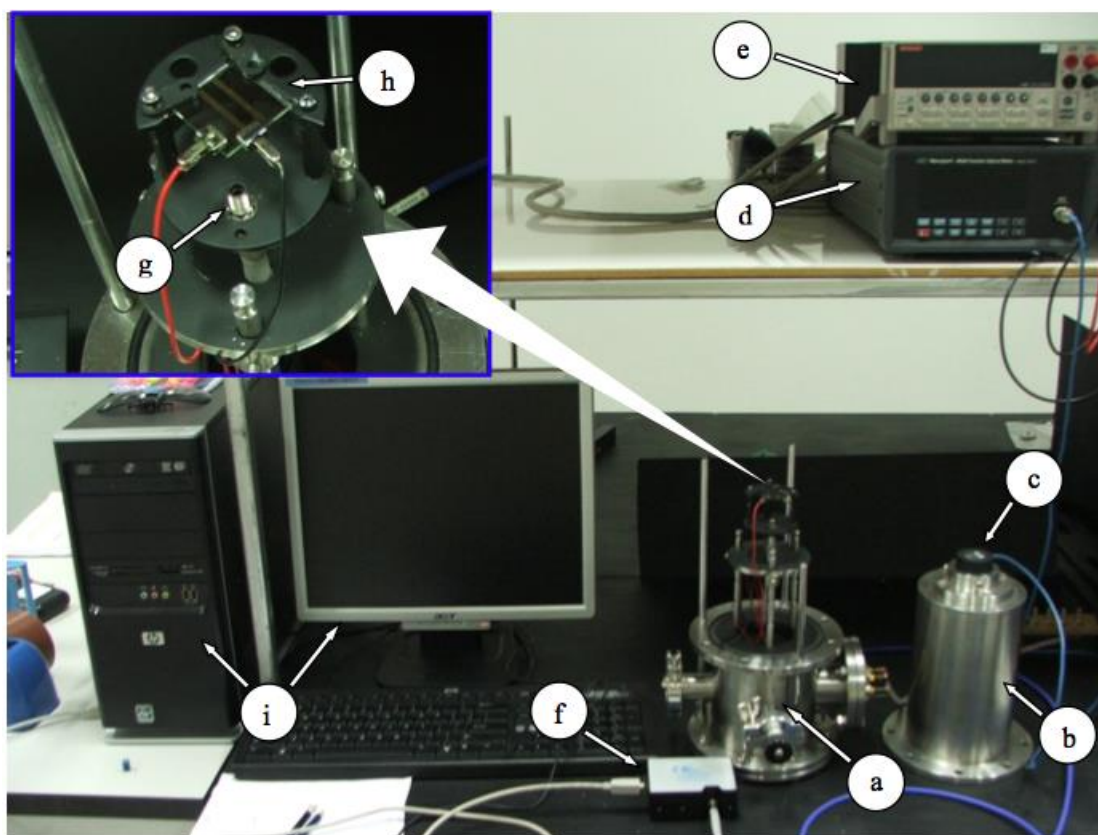


Figure 2.8 Instruments for determination of OLED device performance: (a) OLED test box, (b) lid of OLED test box, (c) calibrated photodiode, (d) multifunction optical meter, (e) digital source meter, (f) USB spectrofluorometer, (g) probe of USB spectrofluorometer, (h) OLED device holder, (i) computer controller and recorder for digital source meter, multifunction optical meter, and USB spectrofluorometer.

All device measurements were performed in an OLED test box by blocking the incident light at room temperature under ambient atmosphere. When voltages were applied, the currents, brightness, and EL spectra were recorded at the

same time to give the current density–voltage–luminance (J - V - L) characteristics and EL spectra. The turn-on voltage was defined at the brightness of 1 cd/m². The current density was calculated as the following formula (1):

$$J = \frac{I}{A} \quad (1)$$

Here, I (mA) is the current and A (cm²) is the pixel active area of the device. The luminous efficiency of the device was calculated as the following formula (2):

$$\eta_{\text{lum}} = \frac{L}{J} \quad (2)$$

Here, L (cd/m²) is the luminance and J (mA/cm²) is the current density.

The external quantum efficiency is defined as [63]

$$\eta_{\text{ex}} = \frac{\text{\# of photons emitted into free space per second}}{\text{\# of electron injected into OLED per second}}$$

The external quantum efficiency of the device was calculated as the following formula (3):

$$\eta_{\text{ex}}(\%) = \frac{5.0 \times 10^3}{(h\nu)\phi(\lambda)} \eta_{\text{lum}} \quad (3)$$

Here, $h\nu$ is the photon energy (in eV) of the emission, and $\phi(\lambda)$ is the photopic luminosity function.

CHAPTER III

RESULTS AND DISCUSSION

3.1 Synthesis

Prior to the synthesis of fluorophores, the truxene core was synthesized by a three-step procedure illustrated in **Figure 3.1**. A dehydration and trimerization of hydro-cinnamic acid with polyphosphoric acid (PPA) for 8 h at 160 °C afforded truxene as a light-yellow solid in 49% yield after recrystallization in toluene. The structure was verified by ¹H-NMR comparison with the data reported in the literature [62].

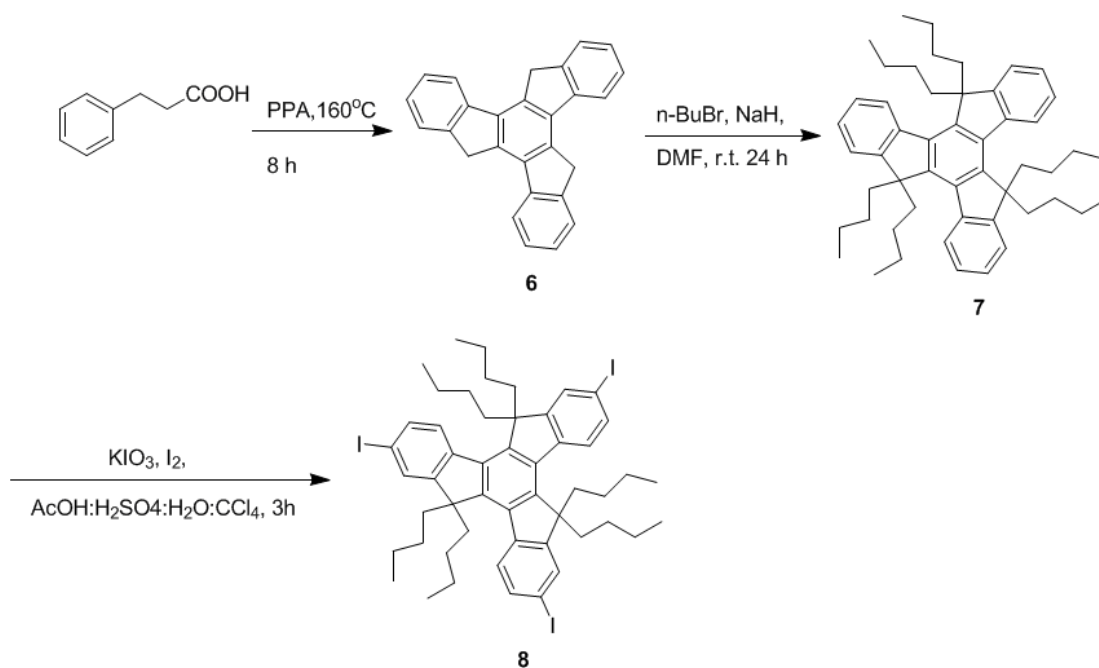


Figure 3.1 The synthesis of **8**

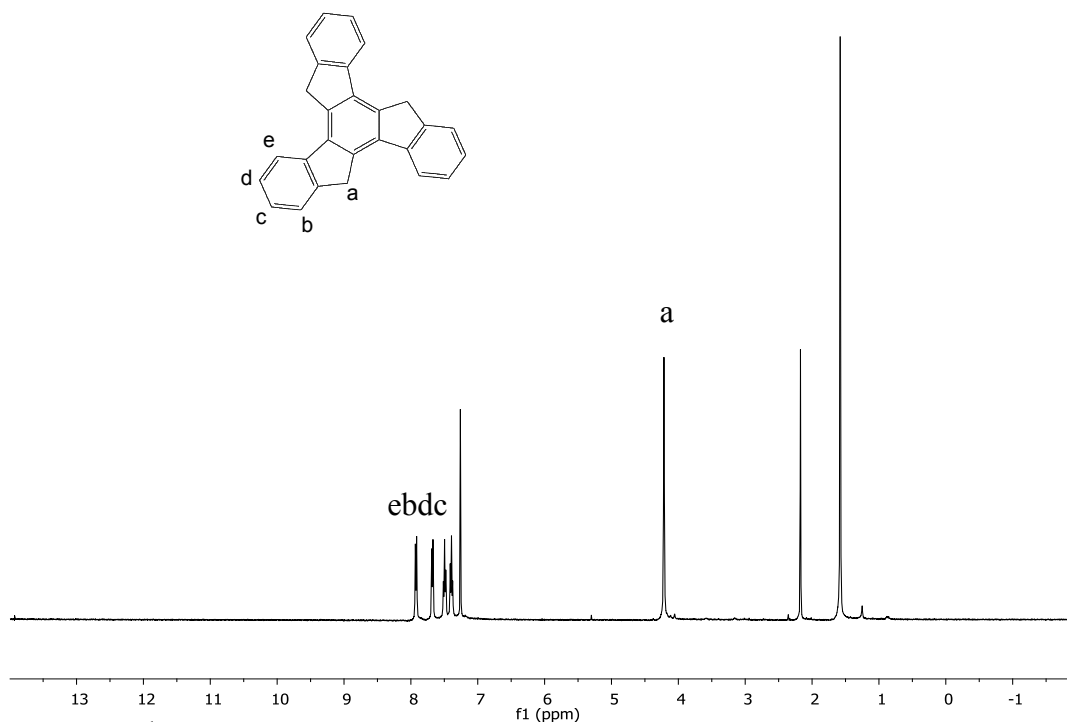


Figure 3.2 $^1\text{H-NMR}$ of **6** in CDCl_3

With the truxene core in hands, the solubility in organic solvent can be enhanced by hexa-alkylation at the position 5,10 and 15 of truxene using NaH and n -butyl bromide in DMF at room temperature with stirring for 24 h. The product was purified by silica gel column chromatography to yield **7** in 75% yield as a white solid.

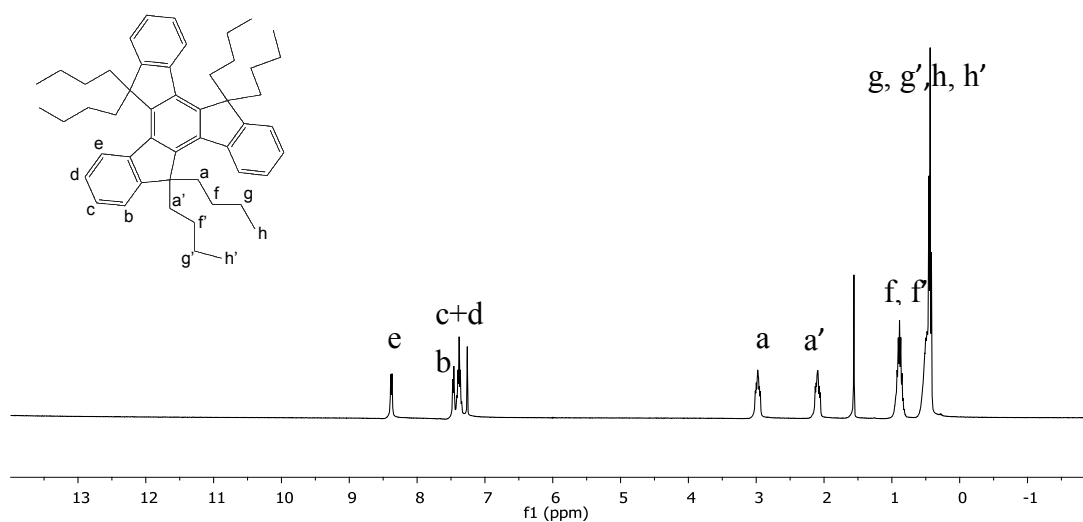


Figure 3.3 $^1\text{H-NMR}$ of **7** in CDCl_3

The regioselective iodination of **7** using KIO_3 and I_2 in solvent mixture between CH_3COOH , H_2SO_4 , H_2O , and CCl_4 gave triiodotruxene **8** in 84% yield as a white solid.

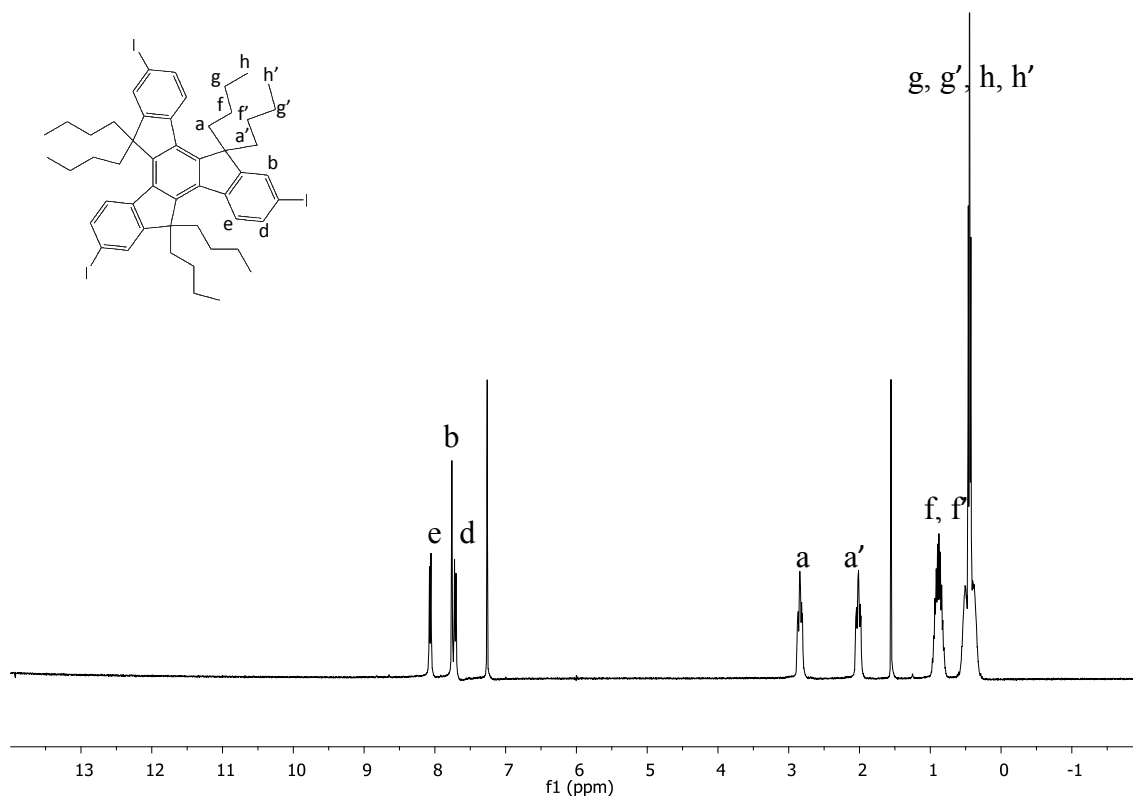


Figure 3.4 $^1\text{H-NMR}$ of **8** in CDCl_3

Meanwhile, the synthesis of the tercarbazoledendron (**5**) involved the regioselective iodination of carbazole at the 3- and 6-positions using KI/KIO_3 in refluxing acetic acid for 20 min to afford 3,6-diiodo-9H-carbazole (**3**) as brown solid in 99% yield after recrystallization[61].

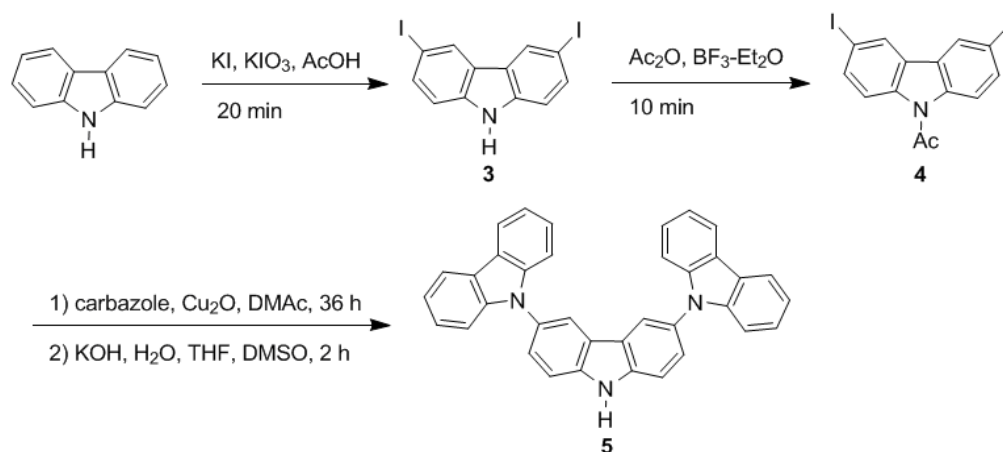


Figure 3.5 The synthesis of tercarbazole dendron (5)

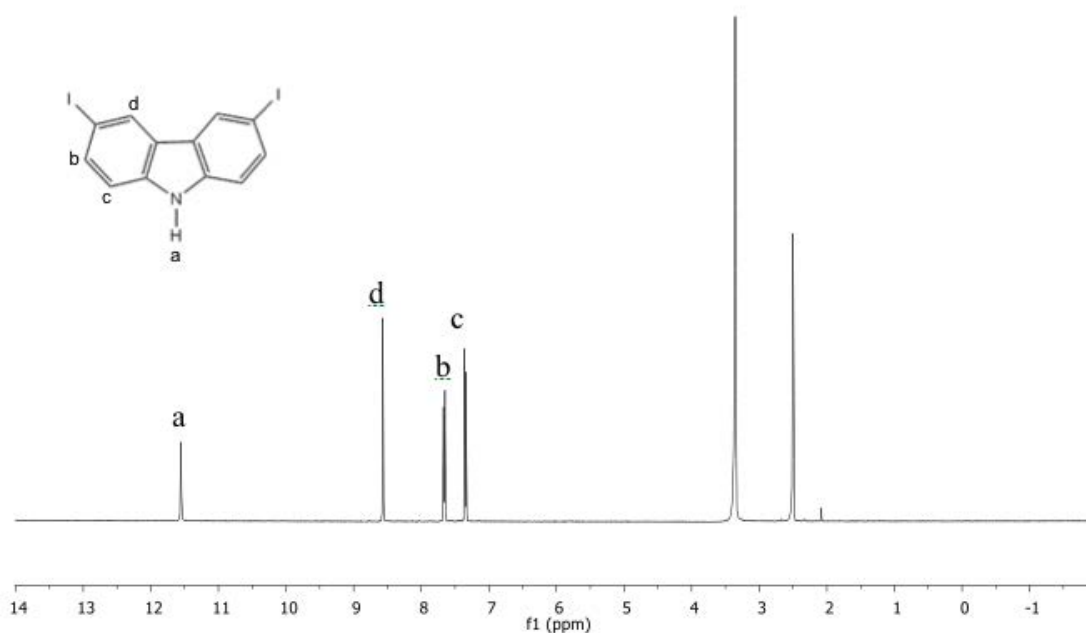


Figure 3.6 ¹H-NMR of 3 in DMSO-*d*₆

To protect the -NH group, the nitrogen in 3,6-diiodo-9H-carbazole (3) was transformed into an amide group using acetic anhydride and boron trifluoride diethyl etherate (BF₃•Et₂O) to give 9-acetyl-3,6-diiodo-carbazole(4) in 92 %yield as a white solid.

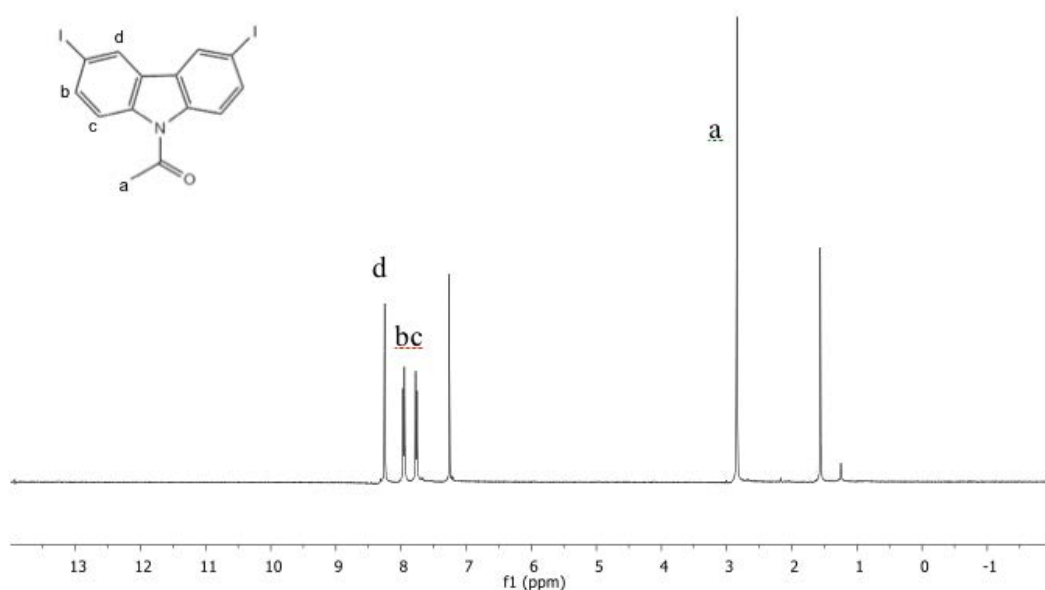


Figure 3.7 ¹H-NMR of **4** in CDCl₃

Eventually, the C-N coupling of between two units of carbazole and diiodo**4** in *N,N*-dimethylacetamide (DMAc) catalyzed by copper(I)oxide (Cu₂O), followed by the hydrolysis of the amide group provided the tercarbazole **5** in 57% for two steps as a white solid.

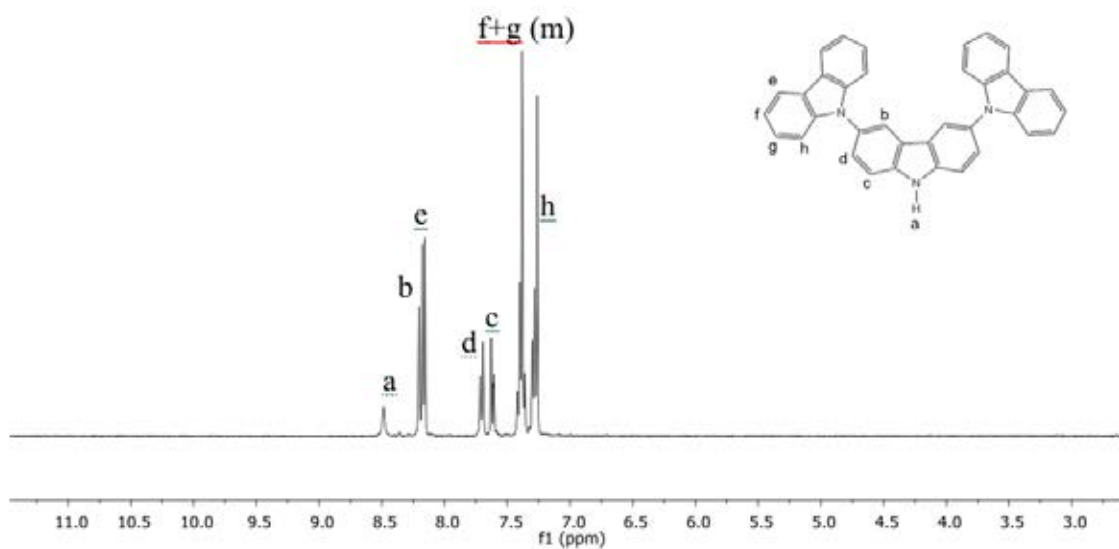


Figure 3.8 ¹H-NMR of **5** in CDCl₃

The mechanism of C-N coupling using Cu as catalyst

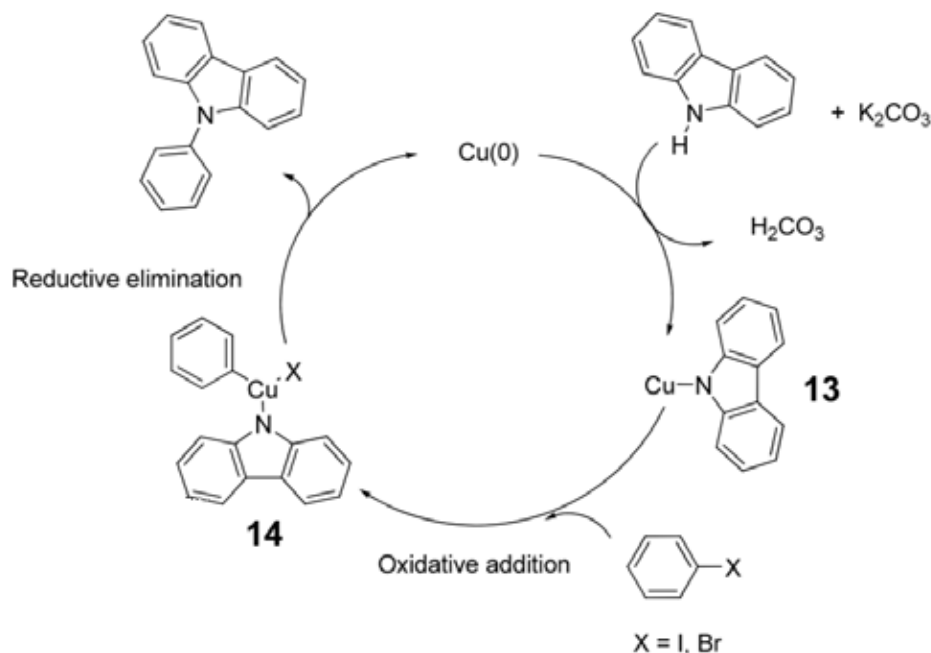


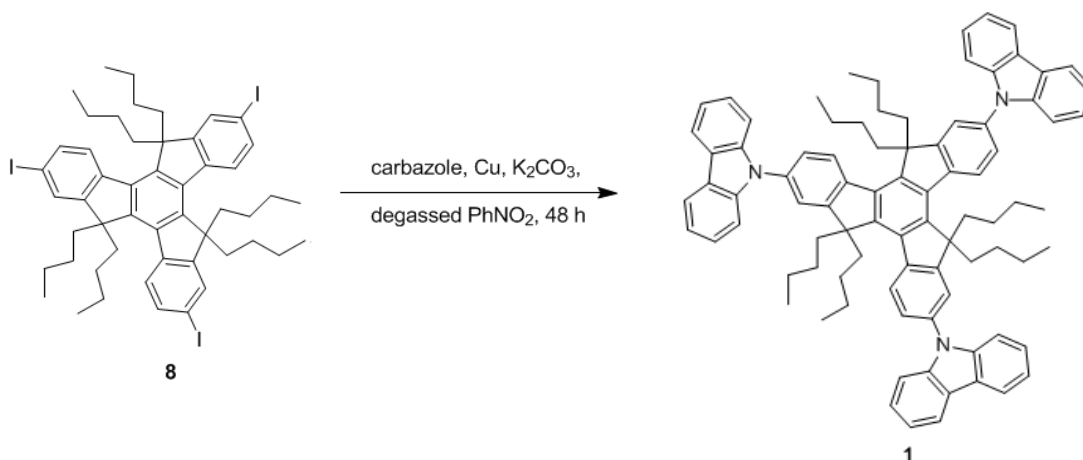
Figure 3.9 The mechanism of Cu-catalyzed C-N coupling reaction

For the preliminary screening of the catalytic system for the synthesis of target molecule **1**, the mixture of CuI and 1,10-phenanthroline were used as catalysts and $CsCO_3$ as a base in DMF (Entry 1, **Table 3.1**). However, this condition did not provide the expected product even when the reaction time was prolonged to 48 h. When Cu powder and K_2CO_3 were used as catalyst and base, the reaction could produce the target compound **1** in unacceptable yield, regardless of the solvent (DMF or $PhNO_2$). However, the yield could be increased when the reaction time was extended from 24 to 48 h or 6 days. We hypothesized that the prolonged reaction time is required as the surface of copper catalyst might be inactive, and the heating and agitation of the mixture could break off the inert surface. These results suggested that the most practical condition was in entry 5. The compound **1** was successfully synthesized as a yellow solid in 40% yield after a silica gel column chromatography.

Table 3.1C-N coupling conditions for compound**1**

Entry	Condition	Time	%yield
1	CuI, 1,10-Phenanthroline, CsCO ₃ DMF, reflux	48 h	-
2	Cu, K ₂ CO ₃ , 18-crown-6 DMF, reflux	24 h	3
3	Cu, K ₂ CO ₃ , DMF, reflux	24 h	6
4	Cu, K ₂ CO ₃ , degassed PhNO ₂ , reflux	24 h	7
5	Cu, K ₂ CO ₃ , degassed PhNO ₂ , reflux	48 h	40
6	Cu, K ₂ CO ₃ , degassed PhNO ₂ , reflux	6 days	51

The synthesis of target compound**1** and **2** is shown in **Figure 3.10** and **Figure 3.11** respectively.

**Figure 3.10** The synthesis of compound**1**

The chemical structure of compound **1** was characterized by ¹H NMR, ¹³C

NMR and MALDI-TOF spectrometry. The ^1H NMR of compound **1** (Figure 3.11) in CDCl_3 showed a doublet peak at 8.5 ppm for H(e), a doublet peak at 8.22 ppm for H(i), a singlet peak at 7.73 ppm for H(b), a doublet peak at 7.66 ppm for H(d), a doublet peak at 7.59 ppm for H(j), a triplet peak at 7.49 ppm for H(k), a triplet peak at 7.35 ppm for H(l) and around 0-3.5 ppm for alkyl chain.

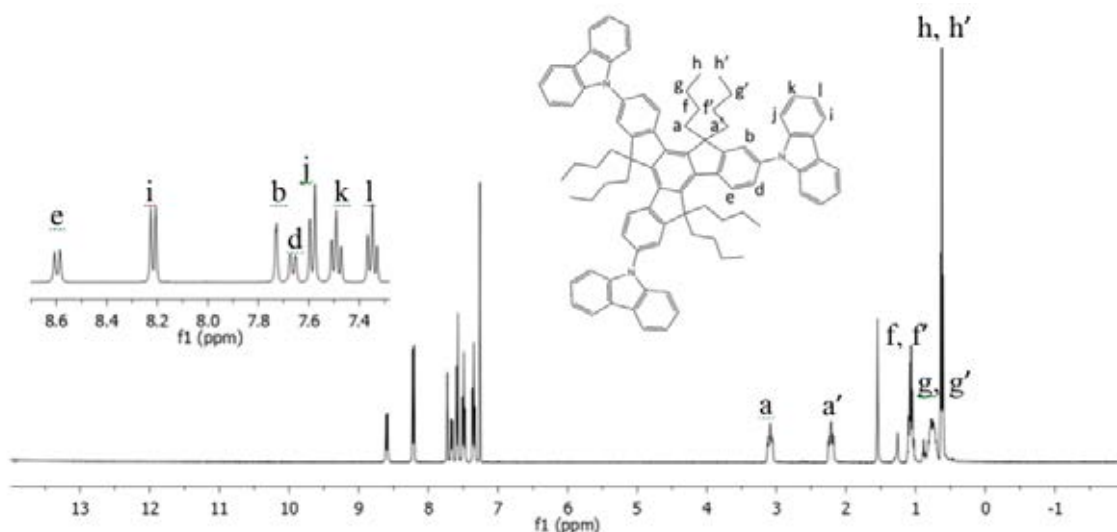


Figure 3.11 ^1H NMR of compound **1** in CDCl_3

The synthesis of compound **2** is shown in Figure 3.12. Compound **2** was synthesized by the reaction of **8** and excess amount of **5** in the presence of Cu bronze and K_2CO_3 in degassed nitrobenzene at refluxing temperature. Compound **2** was obtained by silica gel column chromatography as an orange brown solid in 50% yield.

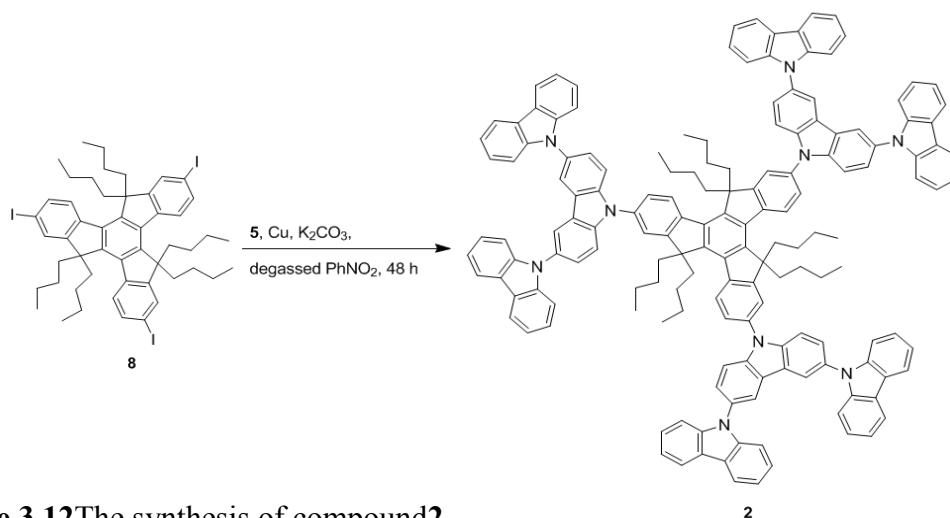


Figure 3.12 The synthesis of compound **2**

The chemical structure of compound **2** was characterized by ^1H NMR, ^{13}C NMR and MALDI-TOF spectrometry. The ^1H NMR of compound **2** (Figure 3.13) in

CDCl_3 showed a doublet peak at 8.80 ppm for H(e), a singlet peak at 8.40 ppm for H(k), a doublet peak at 8.22 ppm for H(o), a singlet peak at 7.99 ppm for H(b) and at around 0-3.5 ppm for alkyl chain.

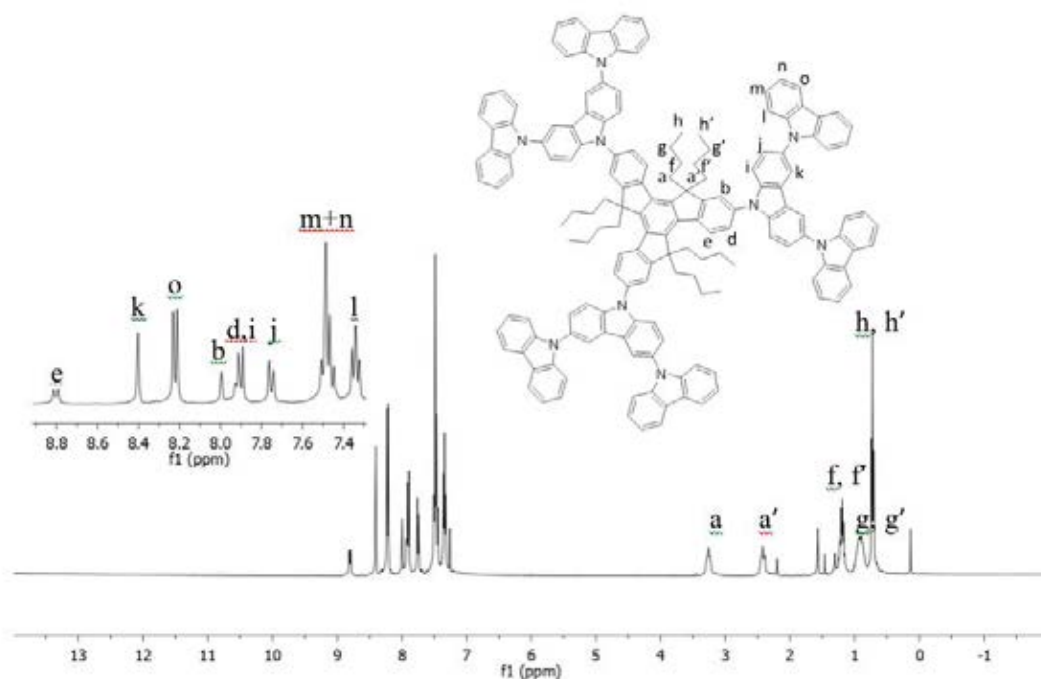


Figure 3.13 ^1H NMR of compound **2** in CDCl_3

3.2 Optical property

The investigation of absorption of compound **1** and **2** were performed in dilute chloroform solution. The normalized absorption spectra are shown in **Figure 3.14** and summarized in **Table 3.2**. The absorption spectra of compound **1** and **2** in solution, showing two strong absorption bands in the visible region at 330 nm corresponding to the π - π^* electron transition of entire conjugated backbone and band at 294 nm corresponding to the π - π^* local electron transition of the carbazole moieties. The similarity of the absorption spectra of compound **1** and **2** showed that the π -conjugation system of both compounds were the same, the equal energy absorbed. This indicated the independent arrangement of molecules in solution phase, each molecule was solvated, the outer carbazole of compound **2** was not included in π -conjugated system because of its steric effect.

Therefore, compound **2** has the same π -conjugated system as compound **1** in this situation. While, thin films were obtained by spin coating method, compound **2** exhibited more bathochromic shift than compound **1** due to better π -electron

delocalization in conjugated systems resulting from better planarity between carbazole dendron, consist of the outer carbazole, and truxene units affected by the solid state packing and prevent aggregation by six-butyl group and bulky nature of carbazole dendron. However, the molar absorptivity of compound **2** was slightly higher than that of compound **1** due to higher number of photoactive carbazole units.

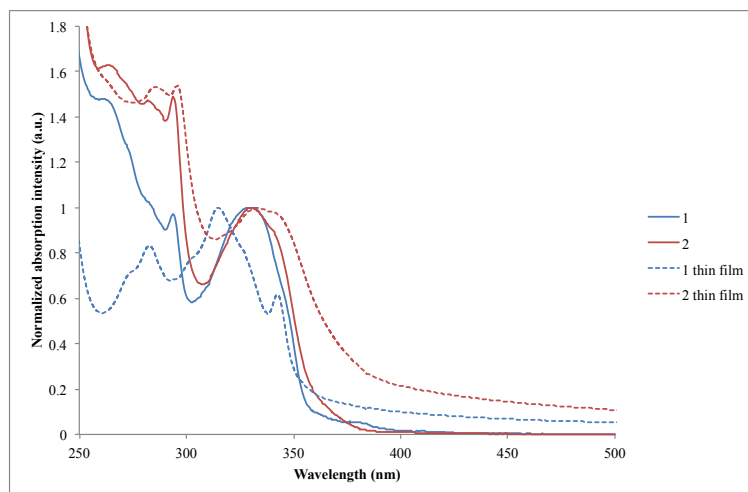


Figure 3.14 Normalized absorption spectra of compound **1,2** in CHCl_3 and thin film

The normalized fluorescence spectra are shown in **Figure 3.15**, obtained from CHCl_3 solution. Compound **1** and **2** exhibited the maximum emission wavelength at 367 and 391 nm, respectively, and displayed a typical vibrational progression pattern of truxene core, while the absorption bands are in the same wavelength. The emission band of compound **2** appeared at a longer wavelength which probably due to a higher degree of geometrical relaxation upon excitation with lower energy. For thin film, both compounds showed more bathochromic shift. This suggested that the resonance effect on carbazole molecule may occurred and also obvious by the lower quantum efficiency of compound **2** (0.10) as compared to that of compound **1** (0.22). The quantum yield was measured in CHCl_3 solution at room temperature using 2-aminopyridine in 0.1 M H_2SO_4 ($\Phi_F = 0.60$) as a standard.

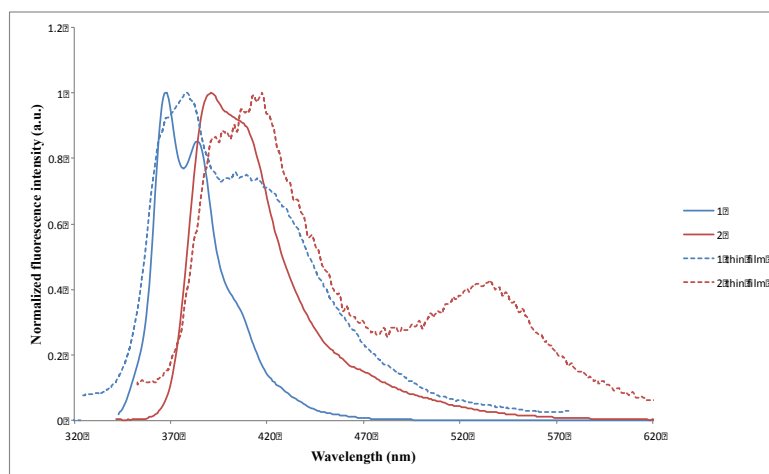


Figure 3.15 Normalized emission spectra of compound **1**, **2** in CHCl_3 and thin film

Table 3.2 Optical properties of compound **1** and **2** measured in CHCl_3 solutions and thin films

Compound	$\lambda_{\text{max}}^{\text{abs}}[\text{nm}]$ ($\log \epsilon [\text{M}^{-1}\text{cm}^{-1}]$)		$\lambda_{\text{max}}^{\text{emit}}[\text{nm}]$		$\Phi_{\text{F}}^{\text{a}}$
	Solution	Thin film	Solution	Thin film	
1	331(4.95)	315	367	379	0.22
2	330(5.05)	333	391	418	0.10

^a 2-aminopyridine in 0.1 M H_2SO_4 ($\Phi_{\text{F}} = 0.60$) was the reference.

3.3 Electrochemical property

From the prior UV-vis experiments, the optical band gap energy could be determined from the onset of absorption wavelength (the lowest energy that molecules absorb to excite the electron to the excited state) was estimated by $E_{\text{g}} = 1240/\lambda_{\text{onset}}$. The onset absorption of compound **1** is 420 nm and compound **2** is 402 nm corresponding to energy band gaps of 2.95 eV and 3.08 eV, respectively.

In this CV experiments, platinum wire was used as a counter electrode, Ag/AgNO_3 as a reference electrode and glassy carbon as a working electrode. *tetra-n-butylammoniumhexafluorophosphate* (TBAPF_6) as a electrolyte which can solute in organic solvents. The concentration of electrolyte was 0.1 M, and the concentration of compound **1** and **2** was 1.0 mM.

The redox potentials were performed in dry dichloromethane at scan rate of 0.05 V/s and result in **Table 3.3**. The cyclic voltammograms of two compounds were showed in **Figure 3.16**. The HOMO energy level of compound **1** and **2** were calculated by an empirical formula, $\text{HOMO} = -(4.44 + E_{\text{onset}})$ (eV)[64,65]. The onsets of oxidation potential of compound **1** and **2** were at 0.75 and 0.63, respectively. These suggested that compound **2** could be oxidized easier and have better hole-transporting property than compound **1**. The LUMO energy level was calculated by HOMO energy level subtracted with the energy band gap from calculation of the onset of UV-Vis absorption.

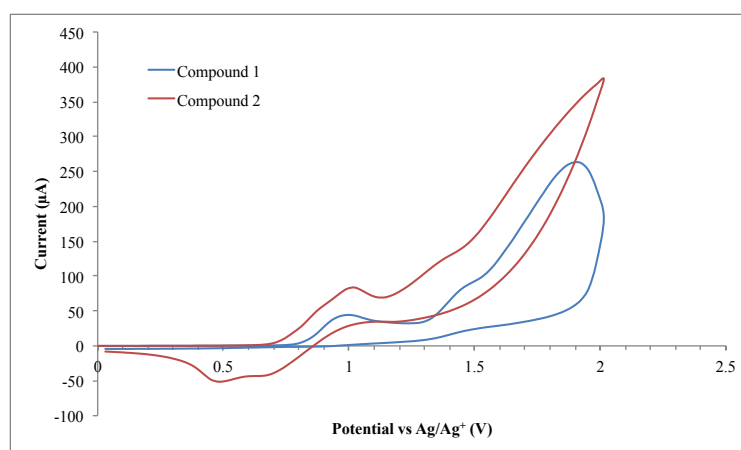


Figure 3.16 The cyclic voltammograms of compound **1** and **2**

Table 3.3 The electrochemical properties of compound **1** and **2**

Compound	HOMO ^b (eV)	LUMO ^c (eV)	E _g ^d (eV)
1	5.19	2.24	2.95
2	5.07	1.99	3.08

^aMeasured using a glassy carbon as a working electrode, a platinum wire as a counter electrode, and Ag/AgNO₃ as a reference electrode in CH₂Cl₂ containing 0.1M TBAPF₆ as a supporting electrolyte at a scan rate of 50 mV/s under a nitrogen atmosphere.

^bCalculated by the empirical equation: $\text{HOMO} = -(4.44 + E_{\text{onset}})$.

^cCalculated from $\text{LUMO} = \text{HOMO} - E_g$.

^dThe optical energy gap estimated from the onset of the absorption spectra ($E_g = 1240/\lambda_{\text{onset}}$).

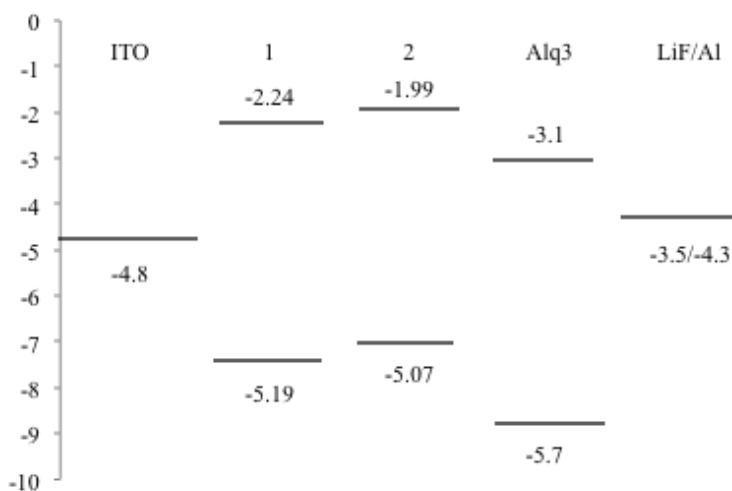


Figure 3.17 Band diagram of ITO, compound1, compound2, Alq₃ and LiF/Al

3.4 Thermal property

For electroluminescent device, the thermal stability is crucial for durability and lifetime of device. The degradation of the device depends on the morphological change of the amorphous organic layer. The thermal properties were observed by thermo gravimetric analysis (TGA) and Differential scanning calorimetry (DSC) under nitrogen atmosphere.

The thermal properties of compound1 and 2 are shown in **Figure 3.18** and summarized in **Table 3.4**. The TGA curves were suggested that all compounds were thermally stable with 5% weight loss temperature (T_{5d}) at 392 and 371 °C, respectively. From DSC on second heating cycle, compound1 showed only an endothermic peak at 249 °C due to glass transition temperature (T_g) and no signal for melting and crystallization temperature was observed. For compound2 showed endothermic baseline shift at due to glass transition temperature (T_g) at 293 °C. These results suggested that all compounds could form molecular glass with high T_g .

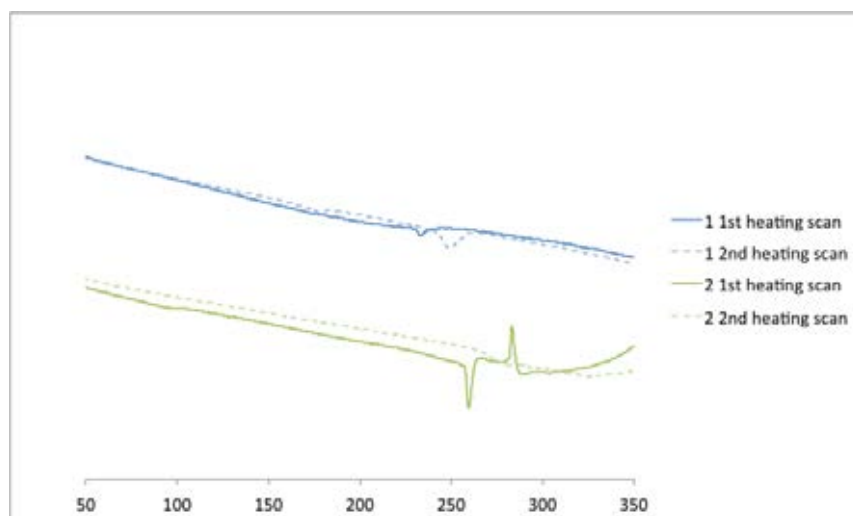


Figure 3.18 DSC curves of compound **1** and **2** at a heating rate of 10 °C/min under N₂ atmosphere

Table 3.4 Thermal properties of compound **1** and **2**.

Compound	mp ^c (°C)	T _g ^a (°C)	T _d ^b (°C)
1	>300	249	392
2	>300	293	371

^aObtained from DSC measurements on the second heating cycle with a heating rate of 10 °C/min under N₂ atmosphere. ^bObtained from TGA measurements with a heating rate of 10 °C/min under N₂ atmosphere.

^c Obtained from scientific melting point

3.5 Hole transporting (HTL) property

3.5.1 Investigation of the hole transporting property

The HOMO energy level of compound **1** and **2** were at 5.19 and 5.07 eV respectively. These energy levels lie between work function of ITO (4.80 eV) and HOMO energy level of Alq₃ (5.70 eV) which indicated that all compounds could be used as HTL in OLED. The barriers between ITO and compound **1** and **2** were 0.49 and 0.37 eV, respectively, that could be suggested that hole injection from ITO to compound **2** could be more easily occurred. The LUMO energy level of compound **1** and **2** were at 2.24 and 1.99 eV, respectively, that higher than LUMO energy level of

Alq₃(3.1 eV). This also suggested that both compounds could be acted as electron blocking materials. Because of high molecular weight of compound **2**, Spin coating method was used instead of thermal evaporation to coated hole transporting layer onto the devices. Multi-layer OLED were fabricated with structure of ITO/HTL[30nm]/Alq₃[40nm]/LiF[0.5nm]/Al[120nm] by using compound **1** and **2** as hole transporting layer. Only device 5, NPB, commercial hole transporting material, was used as HTL to be compared with our compounds. ITO as the anode, LiF/Al as the cathode and Alq₃ as the light emitting and electron transporting layer. All devices emit green color of Alq₃ (530 nm), indicated that compound **1** and **2** were only the hole transporting layer.

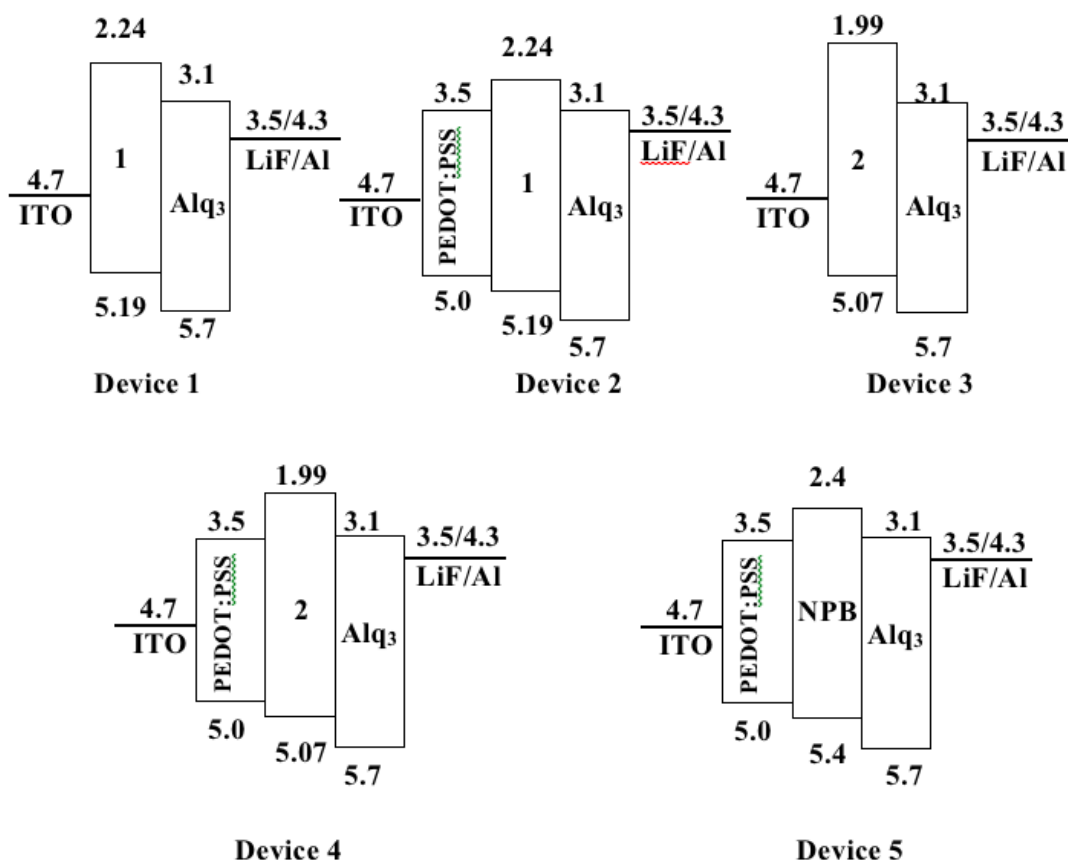


Figure 3.19 Energy level diagram of device 1-5

The voltage-luminance and voltage-current density characteristics of the devices are shown in **Figure 3.20** and summarized in **Table 3.5**. From device 1 and 3, it showed that compound **2** have better hole transporting property than compound **1**. And in the present of PEDOT:PSS as HTM, the performance of device can be improved by effectively control the recombination of hole and electron. Resulting in

decreased turn-on voltage and current density while increased maximum luminescence, luminance efficiency, and external quantum efficiency. Device 4 exhibited the best performance with maximum luminance of 9658 cd/m^2 at 9.2 V, a turn-on voltage of 3.6 V and an external efficiency of 0.056%, due to the lower energy barrier between compound 2 and ITO. Never the less, device 4 exhibited lower performance than device 5 which used NPB, commercial HTM, as HTL.

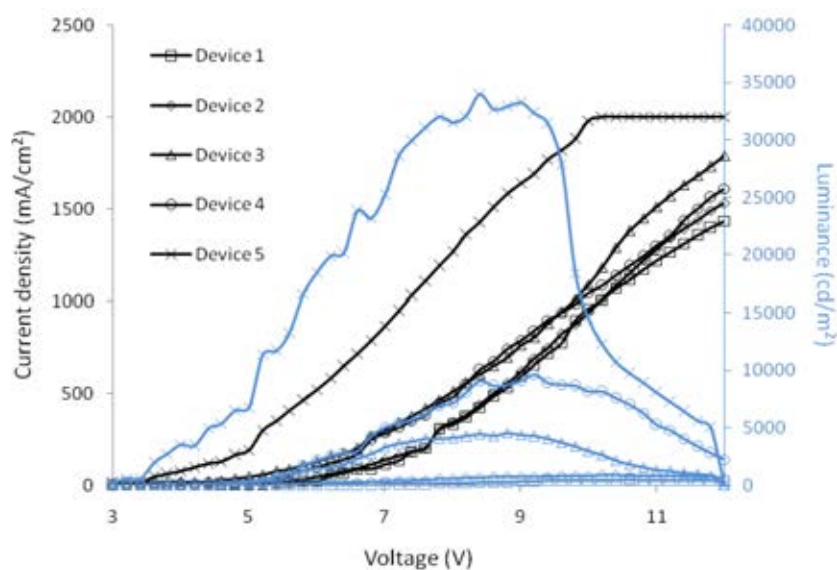


Figure 3.20 Current density and luminance VS voltage characteristic of device 1-5

Table 3.5 Electroluminescent properties of device 1-5

Device	HTL ^f	V _{on} ^a	L _{max} ^b	η_{lum} ^c	η_{ex} ^d	\mathcal{J} ^e
1	1	5.8	454(10.6)	0.04	0.002	1433
2	1 with PEDOT:PSS	4.8	2626(9.2)	0.42	0.021	1329
3	2	3.6	4547(8.8)	0.65	0.031	1786
4	2 with PEDOT:PSS	3.6	9658(9.2)	1.15	0.056	1612
5	NPB with PEDOT:PSS	2.2	33985(8.4)	2.37	0.116	2000

^aTurn-on voltage (V). ^bMaximum luminance (cd/m^2) (at applied potential, V).

^cLuminance efficiency (cd/A). ^dExternal efficiency (%). ^e Current density (mA/m^2)

^fSpin coating method at 2500 rpm for 30 s, concentration of compound=2%w/v

3.5.2 Investigation of thickness of hole transporting layer

To study about the thickness of hole transporting layer, Double-layer OLED was fabricated using compound 2 as hole transporting layer with the structure ITO/PEDOT:PSS[30nm]/HTL/Alq₃[40nm]/LiF[0.5nm]/Al[120nm] by vary the concentration of compound 2 at 1, 2, 3 and 5 %w/v with spin coating method at 2500 rpm for 30s. Device configurations are shown in **Figure 3.21**.

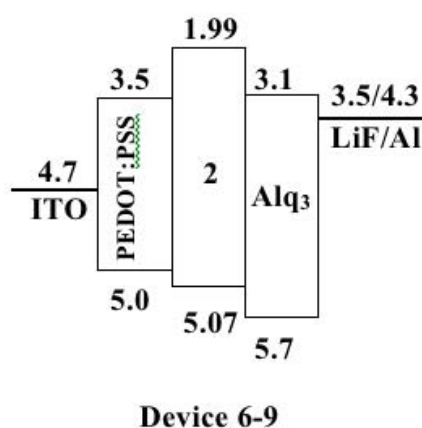


Figure 3.21 Device configuration of device 6-9

The voltage-luminance and voltage-current density characteristics of the devices are shown in **Figure 3.22** and summarized in **Table 3.6**. Device 7 exhibited the best performance with maximum luminance of 9658 cd/m² at 9.2 V, a turn-on voltage of 3.6 V and an external efficiency of 0.056%.

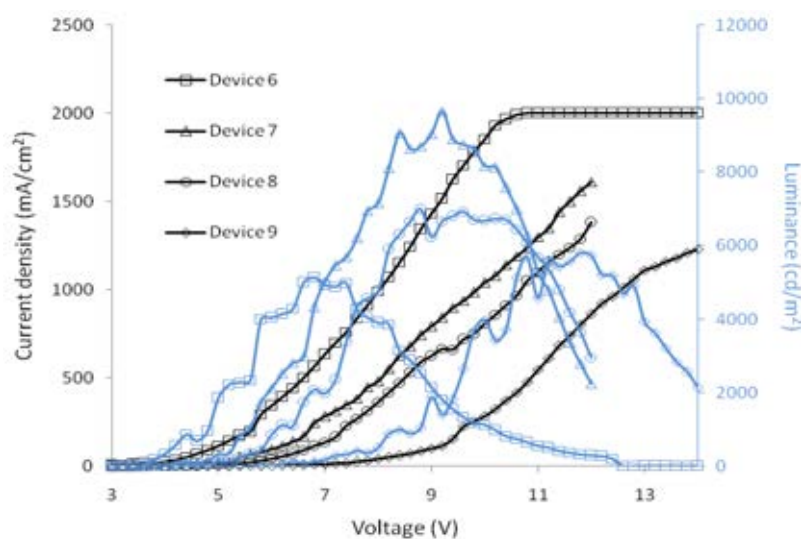


Figure 3.22 Current density and luminance VS voltage characteristic of device 6-9

Table 3.6 Electroluminescent properties of device 6-9

Device	conc. ^f	V _{on} ^a	L _{max} ^b	η _{lum} ^c	η _{ex} ^d	J ^e
6	1	3	5129(6.8)	0.91	0.044	2000
7	2	3.6	9658(9.2)	1.15	0.056	1612
8	3	3.8	6992(8.8)	1.19	0.058	1379
9	5	4	5806(11.8)	0.72	0.035	1226

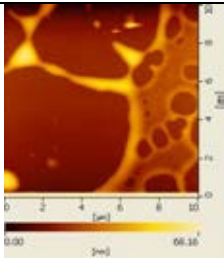
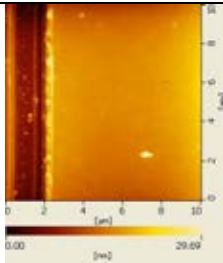
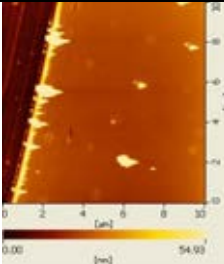
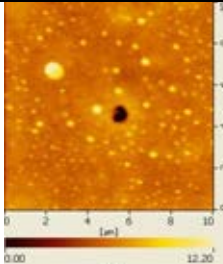
^aTurn-on voltage (V). ^bMaximum luminance (cd/m²) (at applied potential, V).

^cLuminance efficiency (cd/A). ^dExternal efficiency (%). ^eCurrent density (mA/m²)

^fSpin coating method at 2500 rpm for 30 s (%w/v).

The AFM results are shown in **Table 3.7**. At concentration of 1%w/v, the thin film could not be formed. While at concentration 2, 3 and 5 %w/v, thin film could form in a good surface. However, the molecular aggregation was occurred at 3 and 5 %w/v. Therefore, the appropriate condition was the concentration of 2 %w/v. This results corresponding to device performance above. When the concentration was increased, performance of device decreased. This suggested that the recombination of electron and hole in the emitting layer was affected by the thickness of hole transporting layer and also the hole mobility of hole transporting layer (compound **2**)

Table 3.7 AFM image of compound **2** at 1, 2, 3 and 5 %w/v

Conc. (%w/v)	AFM image	Thickness (nm)	Conc. (%w/v)	AFM image	Thickness (nm)
1		Not fully form film	2		14
3		19	5		24

CHAPTER IV

CONCLUSION

Two new hole-transporting materials for OLED were successfully synthesized from carbazole and truxene. The solubilities of these compounds in organic solvents were facilitated and the aggregation by pi-pi stacking was prevented by alkylation at the methylene units of truxene. The iodination of truxene core and Cu-catalyzed C-N coupling with carbazole or 3,6-di(9-carbazolyl) carbazole then gave rise to the target compounds in moderate yields. All compounds were characterized by NMR spectroscopy, UV-Vis and fluorescence spectrophotometry and MALDI-TOF spectrometry. The absorption spectra of both compounds were acquired in CHCl₃ solution and thin film. In solution phase, the compounds displayed maximum absorption and emission wavelengths at 330-331 and 367-391 nm, respectively. The onset absorption of compound **1** is 420 nm and compound **2** is 402 nm, corresponding to energy band gaps of 2.95 eV and 3.08 eV, respectively. On the other hand, they showed absorption at 315-333 and emission at 379-418 nm as thin film state. The quantum yield of compound **1** and **2**, which were measured in CHCl₃ solution using 2-aminopyridine as a standard, were 0.22 and 0.10, respectively. Thermal properties of the compounds were determined by differential scanning calorimetry (DSC) and thermogravimetric analysis (TGA) under nitrogen atmosphere. Both compounds possess excellent thermal stabilities with high glass transition temperatures (T_g) of above 240 °C and decomposition temperature above 370 °C, which is necessary property of good thin film. The electrochemical properties were studied by cyclic and differential pulse voltammetric methods. The HOMO energy level of compound **1** and **2** were at 5.19 and 5.07 eV, respectively. These compounds were fabricated as hole-transporting materials in organic light-emitting devices. The device having the structure of ITO/PEDOT:PSS/2/Alq₃/LiF:Al exhibited a bright green emission with a maximum luminescence of 9,658 cd/m² at 9.2 V and a turn-on voltage of 3.6 V.

REFERENCES

- [1] Zhu, F. OLED activity and technology development. Singapore: Institute of materials research and engineering, 2009.
- [2] Tang, C. W. and VanSlyke, S. A. Organic electroluminescent diodes. Applied Physics Letters 51 (1987) : 913-915.
- [3] Hung, L. S. and Chen, C.H. Recent progress of molecular organic electroluminescent materials and devices. Materials Science and Engineering Reports : A Review Journals 39 (2002) : 143-206.
- [4] Stark, P. and Westling, D. OLED-Evaluation and clarification of the new Organic Light Emitting Display technology. Sweden: Department of Science a Technology, Linköping University, 2002.
- [5] Veinot, J. G. C. and Marks, T. J. Toward the Ideal Organic Light-Emitting Diode: The Versatility and Utility of Interfacial Tailoring by Cross-Linked Siloxane Interlayers. Accounts of Chemical Research 38 (2005) : 632-643.
- [6] Kulkarni, A. P.; Tonzola, C. J.; Babel, A. and Jenekhe, S. A. Electron Transport Materials for Organic Light-Emitting Diodes. Chemistry of Materials 16 (2004) : 4556-4573.
- [7] VanSlyke, S. A.; Chen, C. H. and Tang, C. W. Organic electroluminescent devices with improved stability. Applied Physics Letters 69 (1996) : 2160-2162.
- [8] Halls, J. J. M.; Walsh, C.A.; Greenham, N.C.; Marseglia, E.A.; Friend, R.H.; Moratti, S.C. and Holmes, A.B. Efficient photodiodes from interpenetrating polymer networks. Nature 376 (1995) : 498-500.
- [9] Drury, C. J.; Mutsaers, C. M. J.; Hart, C. M.; Matters, M. and De Leeuw, D. M. Low cost all polymer integrated circuits. Applied Physics Letter 73 (1998) : 108-110.
- [10] Horowitz, G.; Fichou, D.; Peng, X.; Xu, Z. and Garnier, F.A field-effect transistor based on conjugated alphasexithienyl. Solid State Communications 72 (1989) : 381-384.
- [11] Sirringhaus, H.; Tessler, N. and Friend, R. H. Recent Progress in Materials for Organic Electronics. Science 280 (1998) : 1741-1744.

- [12] Bao,Z.;Lovinger, A. and Brown, J. New air-stable n-channel organic thin-film transistors. Journal of the American Chemical Society 120 (1998) : 207.
- [13] Ducharme, S.; Scott, J.C.; Twieg, R.J. and Moerner, W.E. Observation of the photorefractive effect in a polymer. Physical Review Letters. 66 (1991) : 1846-1849.
- [14] Hofmann, U. Optimization of Multilayer Organic Light-Emitting Devices. SPIE International Society for Optical Engineering. 124 (1998) : 3417.
- [15] Meerholtz,K.;Volodin, B.;Sandalphon.;Kippelen, B. and Peyghambarian, N. Advanced Photorefractive and Light-Emitting Organic Materials. Nature 371 (1994) : 497-500.
- [16] Burroughes, J. H.; Bradley, D. D. C.; Brown, A. R.; Marks, R. N.; Mackay, K.; Friend, R. H.; Burns, P. L. and Holmes, A. B. Light-emitting diodes based on conjugated polymers. Nature 347 (1990) : 539 – 541.
- [17] Braun, D. and Heeger, A.J. Visible light emission from semiconducting polymer diodes.Applied Physics Letters58 (1991) :1982-1984.
- [18] Braun, D. and Heeger, A.J. Electroluminescence from light-emitting diodes fabricated from conducting polymers. Thin Solid Films 216 (1992) : 96-98.
- [19] Giro, G.;Cocchi, M.; Di Marco, P.; Di Nicolò, E.;Fattori, V.;Kalinowski,J. and Ghedini, M. The role played by cell configuration and layer preparation in LEDs based on hydroxyquinoline metal complexes and a triphenyl-diamine derivative (TPD). Synthetic Metals 102 (1999) : 1018-1019.
- [20] Fang, Q.;Xu, B.; Jiang, B.; Fu, H.; Zhu, W.; Jiang, X. and Zhang, Z. A novel fluorine derivative containing four triphenylamine groups: Highly thermostable blue emitter with hole-transporting ability for organic light-emitting diode (OLED). Synthetic Metals. 155 (2005) : 206-210.
- [21] Sharma, A.; Singh, D.;Makrandi, J.K.;Kamalasanan, M.N.;Shrivastva, R. and Singh, I.Fabrication and characterization of OLED with Mg complex of 5-chloro-8-hydroxyquinoline as emission layer. Materials Chemistry and Physics. 108 (2008) : 179-183.

- [22] Son, S.-H.; Yun, J.-J.; Oh, G.-C.; Jung, S.-Y.; Kim, Y.-K.; Kuhta, A.V.; Olkhovik, V. K.; Sasnouski, G. and Han, E.-M. Electroluminescence characteristics of a novel biphenyl derivative with benzoxazole for organic light-emitting diodes. Current Applied Physics 5 (2005) : 75-78.
- [23] Ko, C.W.; Tao, Y.T. 9,9-Bis{4-[di-(*p*-biphenyl)aminophenyl]}fluorene: a high T_g and efficient hole-transporting material for electroluminescent devices. Synthetic Metals 126 (2002) : 37.
- [24] Ren, X.; Alleyne, B.D.; Djurovich, P.I.; Adachi, C.; Tsyba, I.; Bau, R. and Thompson, M.E. Organometallic Complexes as Hole-Transporting Materials in Organic Light-Emitting Diodes. Inorganic Chemistry 43 (2004) : 1697-1707.
- [25] Chen, C.-H.; Shen, W.-J.; Jakka, K. and Shu, C.-F. Synthesis and characterization of spiro(adamantane-2,9'-fluorene)-based triaryldiamines: thermally stable hole-transporting materials. Synthetic Metals 143 (2004) : 215-220.
- [26] Zhi-feng, Z.; Zhen-bo, D.; Dong, G.; Chun-jun, L. and Peng, L. Improved performance of organic light-emitting devices with 2-(4-biphenyl)-5-(4-butylphenyl)-1,3,4-oxadiazole. Displays. 26 (2005) : 133-136.
- [27] Kao, P.-C.; Chu, S.-Y.; You, Z.-X.; Liou, S.J. and Chuang C.-A. Improved efficiency of organic light-emitting diodes using CoPc buffer layer. Thin Solid Films. 498 (2006) : 249-253.
- [28] Tong, Q.-X.; Lai, S.-L.; Chan, M.-Y.; Lai, K.-H.; Tang, J.-X.; Kwong, H.-L.; Lee, C.-S. and Lee, S.-T. High T_g Triphenylamine-Based Starburst Hole-Transporting Material for Organic Light-Emitting Devices. Chemistry of Materials. 19 (2007) : 5851-5855.
- [28a] Qiu, Y. and Qiao, J. Photostability and morphological stability of hole transporting materials used in organic electroluminescence. Thin Solid Films. 372 (2000) : 265-270.
- [29] Lacowicz, J. Principles of Fluorescence Spectroscopy 3rd Ed. Springer Science, pp 1-25, New York, 2006.
- [30] Chen, C.-T. Evolution of Red Organic Light-Emitting Diodes: Materials and Devices. Chemistry of Materials. 16 (2004) : 4389-4400.

- [31] Mu, H.; Li, W.; Jones, R.; Steckl, A. and Klotzkin, D. A comparative study of electrode effects on the electrical and luminescent characteristics of Alq₃/TPD OLED: Improvements due to conductive polymer (PEDOT) anode. Journal of Luminescence. 126 (2007) : 225-229.
- [32] Fang, Q.; Xu, B.; Jiang, B.; Fu, H.; Zhu, W.; Jiang, X. and Zhang, Z. A novel fluorene derivative containing four triphenylamine groups: Highly thermostable blue emitter with hole-transporting ability for organic light-emitting diode (OLED). Synthetic Metals. 155 (2005) : 206-210.
- [33] Pei, Q. and Yang, Y. Efficient Photoluminescence and Electroluminescence from a Soluble Polyfluorene. Journal of the American Chemical Society. 118 (1996) : 7416-7417.
- [34] Grice, A. W.; Bradley, D. D. C.; Bernius, M. T.; Inbasekaran, M.; Wu, W. W. and Woo, E. P. High brightness and efficiency blue light-emitting polymer diodes. Applied Physics Letters. 73 (1998) : 629.
- [35] Kalyani, N. T.; Dhoble, S. J. Organic light emitting diodes: Energy saving lighting technology—A review. Renewable and Sustainable Energy Reviews. 16 (2012) : 2696–2723.
- [36] Zhao, T.; Liu, Z.; Song, Y.; Xu, W.; Zhang, D. and Zhu, D. Novel Diethynylcarbazole Macrocycles: Synthesis and Optoelectronic Properties. Journal of Organic Chemistry. 71 (2006) : 7422-7432.
- [37] Thomas, K. R. J.; Lin, J. T.; Tao, Y.-T. and Ko, C.-W. Light-Emitting Carbazole Derivatives: Potential Electroluminescent Materials. Journal of the American Chemical Society. 123 (2001) : 9404-9411.
- [38] Kundu, P.; Thomas, K. R. J.; Lin, J. T.; Tao, Y.-T. and Chien, C.-H. High-T_g Carbazole Derivatives as Blue-Emitting Hole-Transporting Materials for Electroluminescent Devices. Advanced Functional Materials. 13 (2003) 445-452.
- [39] Agarwal, N.; Nayak, P. K.; Ali, F.; Patankar, M. P.; Narasimhan, K. L. and Periasamy, N. Tuning of HOMO levels of carbazole derivatives: New molecules for blue OLED. Synthetic Metals. 161 (2011) : 466–473.

- [40] Fu, Y.; Li, Y.; Li, J.; Yan, S. and Bo, Z. High Molecular Weight Dendronized Poly(fluorene)s with Peripheral Carbazole Groups: Synthesis, Characterization, and Properties. Macromolecules. 37 (2004) : 6395-6400.
- [41] Loiseau, F.; Campagna, S.; Hameurlaine, A. and Dehaen, W. Dendrimers Made of Porphyrin Cores and Carbazole Chromophores as Peripheral Units. Absorption Spectra, Luminescence Properties, and Oxidation Behavior. Journal of the American Chemical Society. 127 (2005) : 11352–11363.
- [42] Promarak, V.; Ichikawa, M.; Meunmart, D.; Sudyoadsuk, T.; Saengsuwan, S. and Keawin, T. Synthesis and properties of stable amorphous hole-transporting molecules for electroluminescent devices. Tetrahedron Letters. 47 (2006) : 8949-8952.
- [43] Promarak, V.; Ichikawa, M.; Sudyoadsuk, T.; Saengsuwan, S.; Jungstittiwong, S. and Keawin, T. Synthesis of electrochemically and thermally stable amorphous hole-transporting carbazole dendronized fluorene. Synthetic Metals. 157 (2007) : 17-22.
- [44] Shih, P.-I.; Chiang, C.-L.; Dixit, A.K.; Chen, C.-K.; Yuan, M.-C.; Lee, R.-Y.; Chen, C.-T.; Diao, E.W.-G. and Shu, C.-F. Novel Carbazole/Fluorene Hybrids : Host Materials for Blue Phosphorescent OLEDs. Organic Letters. 8(2006) : 2799-2802.
- [45] Lu, J.; Xia, P.F.; Lo, P.K.; Tao, Y. and Wong, M.S. Synthesis and Properties of Multi Triarylamine-Substituted Carbazole-Based Dendrimers with an Oligothiophene Core for Potential Applications in Organic Solar Cells and Light-Emitting Diodes. Chemistry of Materials. 18 (2006) : 6194-6203.
- [46] Wagner, J.; Pielichowski, J.; Hirsch, A.; Pielichowski, K.; Bogdal, D.; Pajda, M.; Kurek S.S. and Burczyk, A. New carbazole-based polymers for dye solar cells with hole-conducting polymer. Synthetic Metals. 146 (2004): 159-165.
- [47] Promarak, V.; Punkvuang, A.; Sudyoadsuk, T.; Saengsuwan, S.; Jungstittiwong, S. and Keawin, T. Synthesis, optical, electrochemical, and thermal properties of α, α' -bis(9,9-bis-*n*-hexylfluorenyl)-substituted oligothiophenes. Tetrahedron Letters. 48 (2007) : 3661-3665.

- [48] Thaengthong, A.; Saengsuwan, S.; Jungsuttiwong, S.; Keawin, T.; Sudyoadsuk, T.; and Promarak, V. Synthesis and characterization of high Tg carbazole-based amorphous hole-transporting materials for organic light-emitting devices. Tetrahedron Letters. 52 (2011) : 4749–4752.
- [49] Kumchoo, T.; Promarak, V.; Sudyoadsuk, T.; Sukwattanasinitt, M.; Rashatasakhon, P. Dipyrrenylcarbazole derivatives for blue organic light-emitting diodes. Chemistry an Asian Journal. 5(2010) : 2162-2167.
- [50] Promarak, V.; Ichikawa, M.; Sudyoadsuk, T.; Saengsuwan, S.; Jungsuttiwong, S.; Keawin, T. Thermally and electrochemically stable amorphous hole-transporting materials based on carbazole dendrimers for electroluminescent devices. Thin Solid Films. 516 (2008) : 2881–2888.
- [51] Yuan, M.-S.; Wang, Q.; Wang, W.-J.; Li, T.-B.; Wang, L.; Deng, W.; Du, Z.-T. and Wang, J.-R. Symmetrical and asymmetrical (multi)branched truxene compounds: Structure and photophysical properties. Dyes and Pigments. 95 (2012) : 236-243.
- [52] Zong, X.; Liang, M.; Fan, C.; Tang, K.; Li, G.; Sun, Z. and Xue, S. Design of truxene-based organic dyes for high-efficiency dye-sensitized solar cells employing cobalt redox shuttle. The Journal of Physical Chemistry C. 116 (2012) : 11241-11250.
- [53] Wang, Y.; Tsiminis, G.; Yang, Y.; Ruseckas, A.; Kanibolotsky, A.L. Perepichka, I.F.; Skabara, P.J.; Turnbull, G.A. and Samuel, I.D.W. Broadly tunable deep blue laser based on a star-shaped oligofluorene truxene. Synthetic Metals. 160 (2010) : 1397–1400.
- [54] Yua, S.-C.; Sun, Q.; Lei, T.; Du, B.; Li, Y.-F. and Pei, J. Star-shaped oligo(fluorine ethynylene)-functionalized truxene derivatives: synthesis, characterization, and their size effects. Tetrahedron. 65 (2009) : 4165–4172.
- [55] Cao, X.-Y.; Zhou, X.-H.; Zi, H. and Pei, J. Novel Blue-Light-Emitting Truxene Containing Hyperbranched and Zigzag Type Copolymers: Synthesis, Optical Properties, and Investigation of Thermal Spectral Stability. Macromolecules. 37 (2004) : 8874-8882.

- [56] Xia, H.; He, J.; Xu, B.; Wen, S.; Li, Y. and Tian, W. A facile convergent procedure for the preparation of triphenylamine-based dendrimers with truxene cores. Tetrahedron. 64 (2008) 5736–5742.
- [57] Yang, Z.; Xu, B.; He, J.; Xue, L.; Guo, Q.; Xia, H. and Tian, W. Solution-processable and thermal-stable triphenylamine-based dendrimers with truxene cores as hole-transporting materials for organic light-emitting devices. Organic Electronics 10 (2009) : 954–959.
- [58] Williams, A. T. R.; Winfield, S. A. and Miller, J. N. Relative fluorescence quantum yields using a computer controlled luminescence spectrometer. Analyst 108 (1983) : 1067.
- [59] Rusakomicz, R. and Testa, A.C. 2-Aminopyridine as a Standard for Low-Wavelength Spectrofluorimetry. The Journal of Physical Chemistry. 72 (1968) : 2680-2681.
- [60] Warf, A. Negative Dryfilm Photo resist manual. Negative Dryfilm [Online]. 2004. Available from : <http://www.warf.com.html> [2004, May]
- [61] Kimoto, A.; Cho, J. S.; Higuchi, M. and Yamamoto, K. Synthesis of asymmetrically arranged dendrimers with a carbazole dendron and a phenylazomethine dendron. Macromolecules. 37 (2004) : 5531-5537.
- [62] Earmrattana, N.; Sukwattanasinitt, M. and Rashatasakhon, P. Water-soluble anionic fluorophores from truxene. Dyes Pigments. 93 (2012) : 1428-1433.
- [63] Müllen, K. and Scherf, U. Organic light emitting devices. Synthesis, Properties and Application. WILEY-VCH verlag GmbH & Co. KGaA, pp 19, Weinheim, 2006.
- [64] Yang, F.; Zhang, X.L.; Sun, K.; Xiong, M.J.; Xia, P.F.; Cao, Z.J.; Li, Z.H. Enhanced electroluminescent properties of triarylamine-encapped X-branched oligofluorene. Synthetic Metals 158 (2008) : 988–992.
- [65] Zhu, W.; Hu, M.; Yao, R. and Tian, H. A novel family of twisted molecular luminescent materials containing carbazole unit for single-layer organic electroluminescent devices. Journal of Photochemistry and Photobiology A: Chemistry 154 (2003) : 169–177.

APPENDIX

APPENDIX

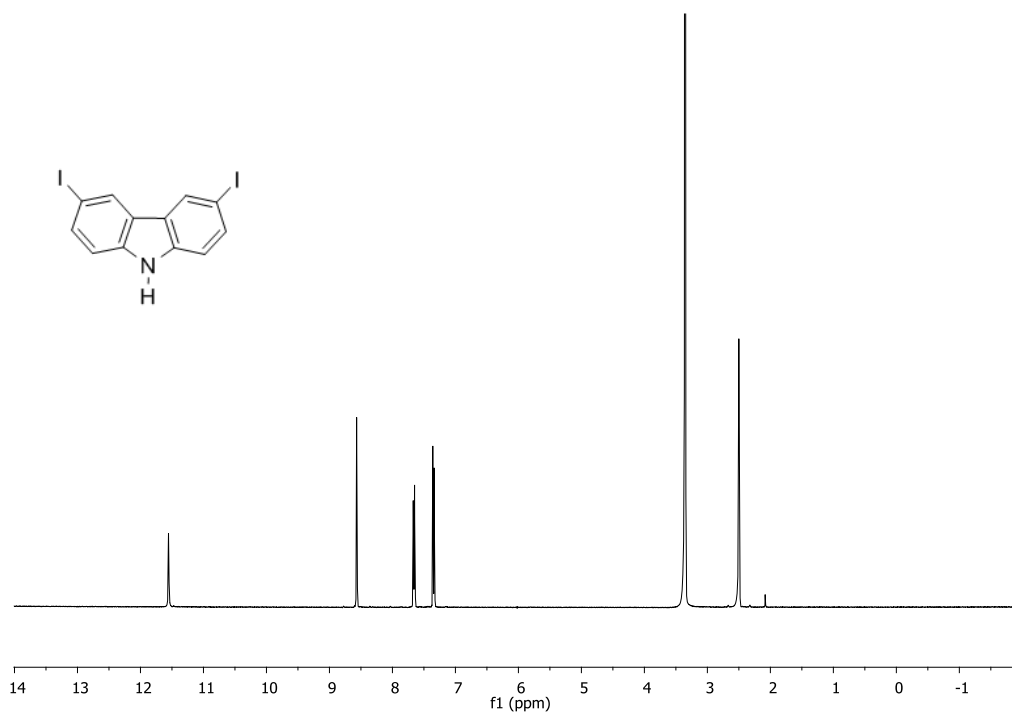


Figure 1 ¹H-NMR spectrum of 3,6-diiodo-9H-carbazole(3)

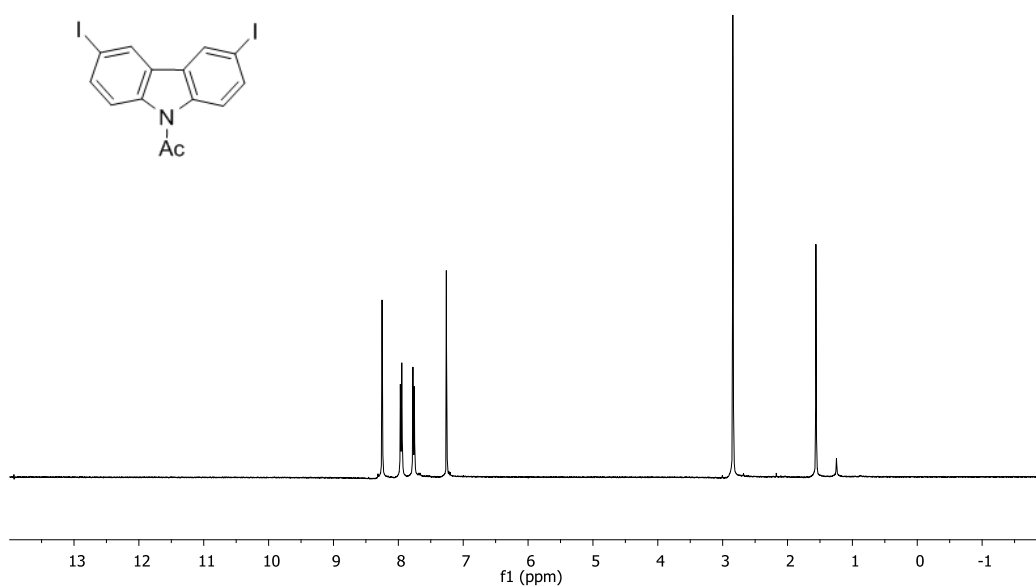


Figure 2 ¹H-NMR spectrum of 9-acetyl-3,6-diiodo-carbazole(4)

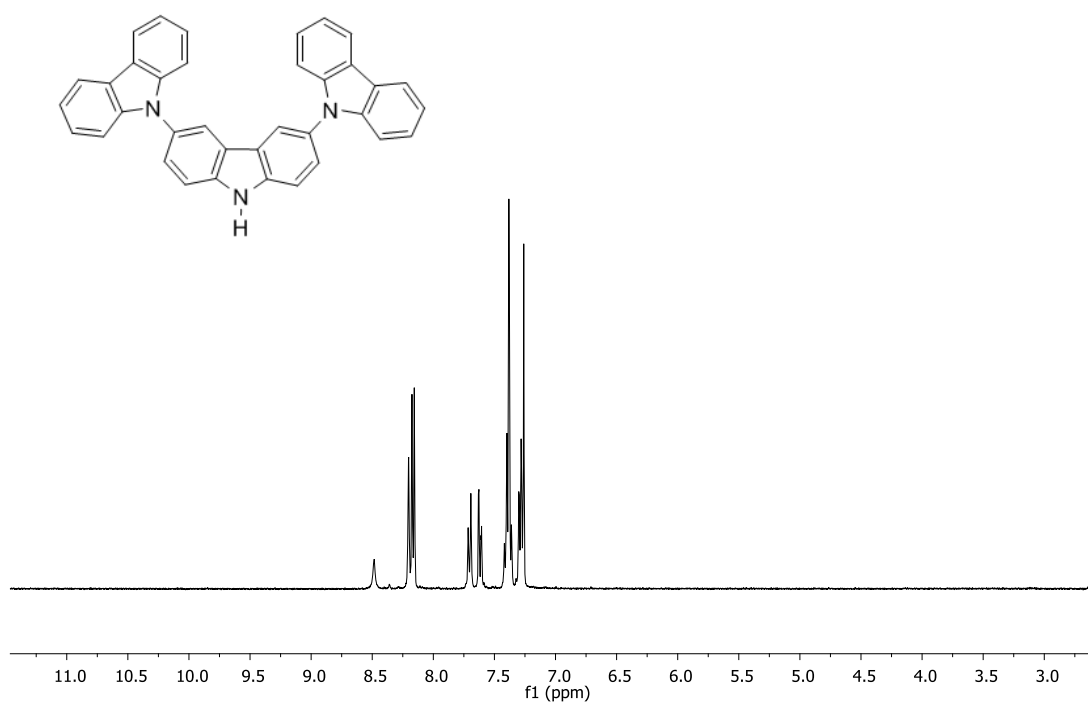


Figure 3 $^1\text{H-NMR}$ spectrum of 3,6-di(9-carbazolyl) carbazole (**5**)

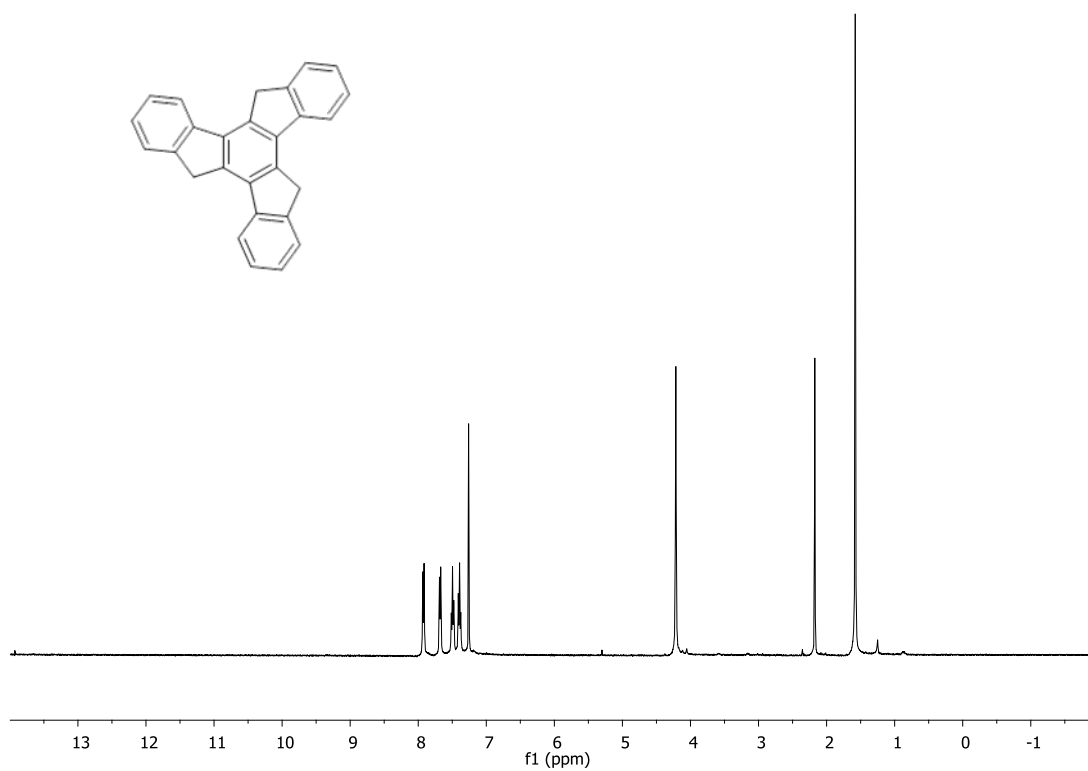


Figure 4 $^1\text{H-NMR}$ spectrum of truxene (**6**)

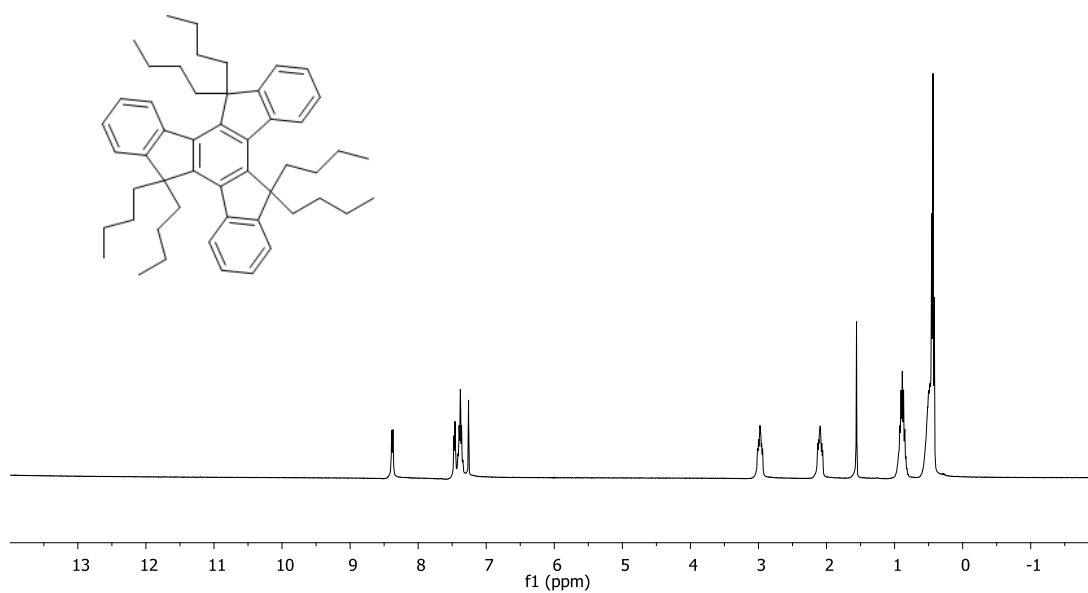


Figure 5 $^1\text{H-NMR}$ spectrum of 5,5,10,10,15,15-hexabutyl-truxene(7)

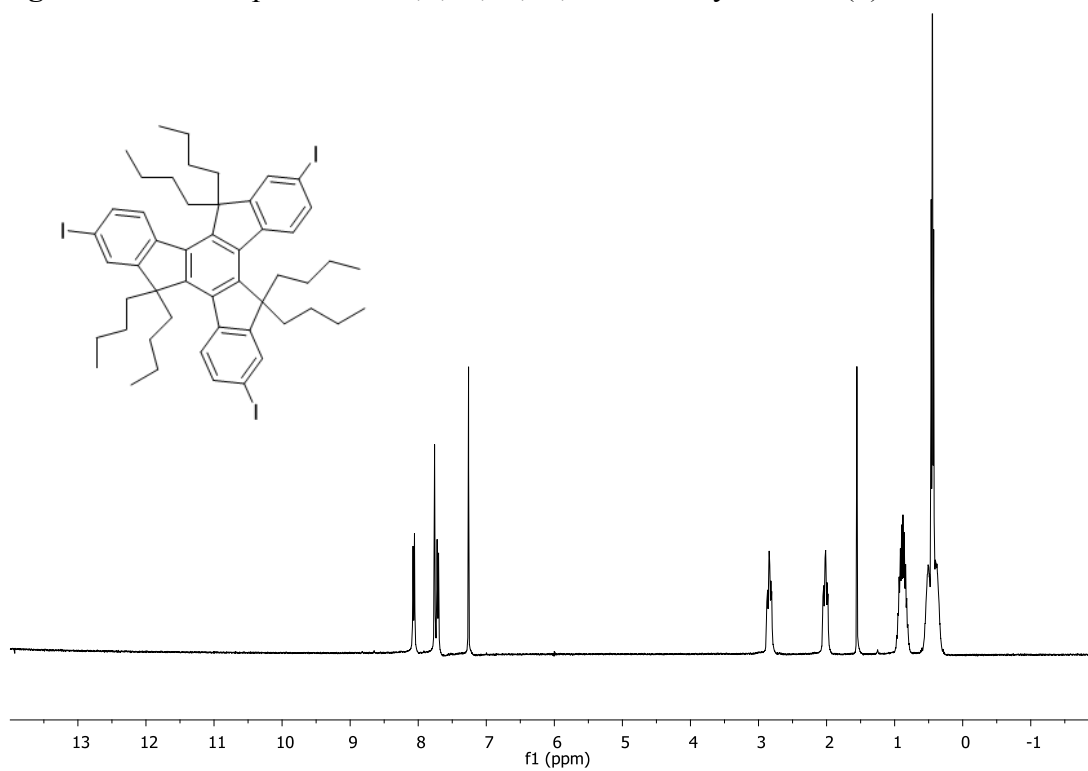


Figure 6 $^1\text{H-NMR}$ spectrum of 5,5,10,10,15,15-hexabutyl-2,7,12-triiodo-truxene (8)

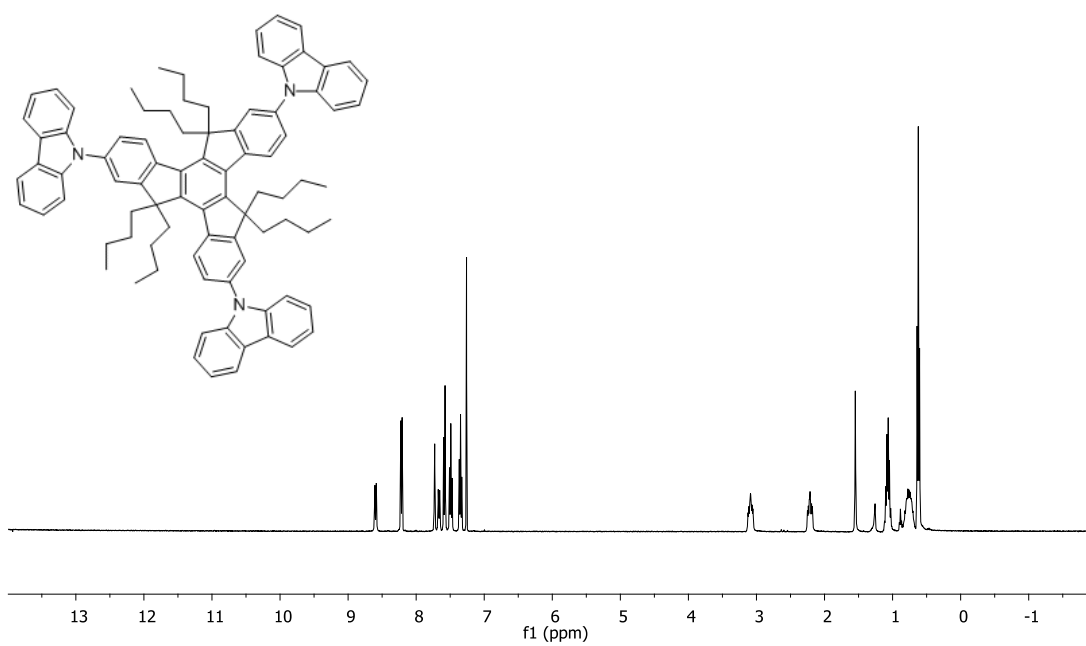


Figure 7 $^1\text{H-NMR}$ spectrum of compound 1

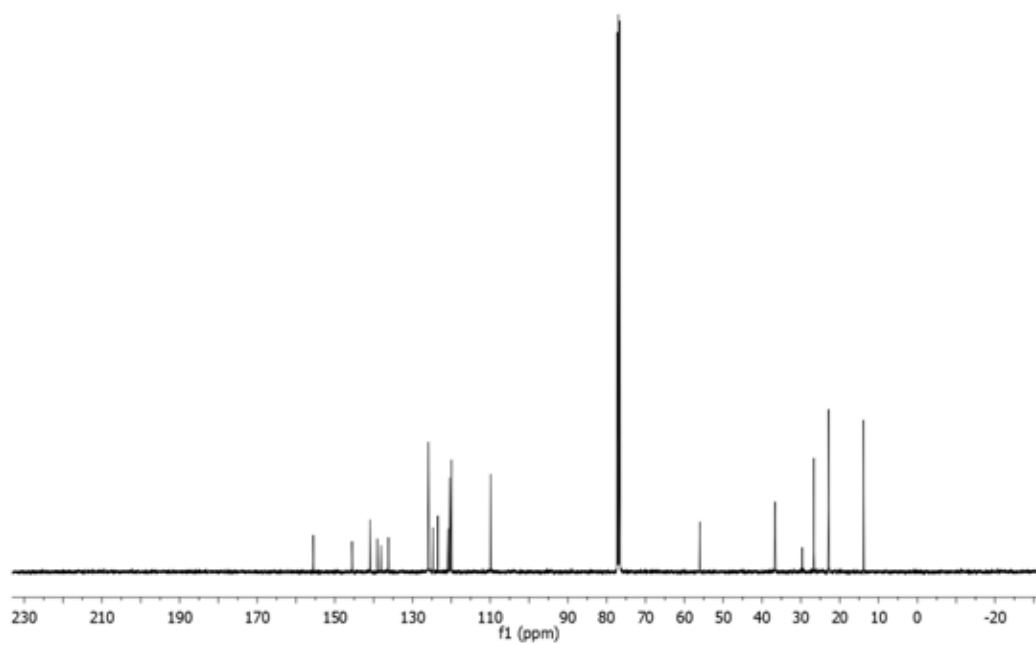


Figure 8 $^{13}\text{C-NMR}$ spectrum of compound 1

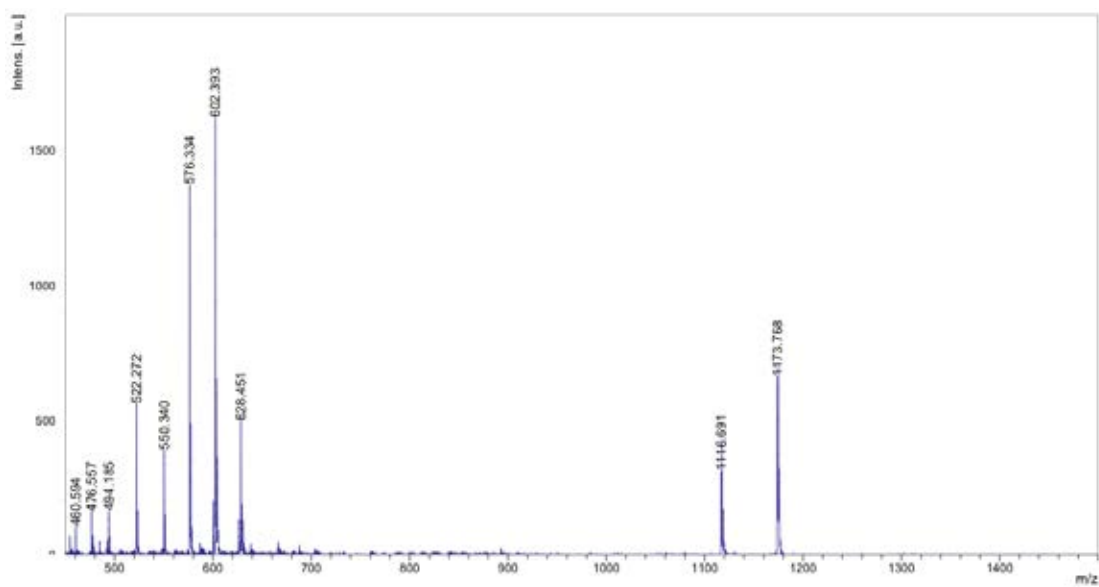


Figure 9 MALDI-TOF spectrum of compound 1

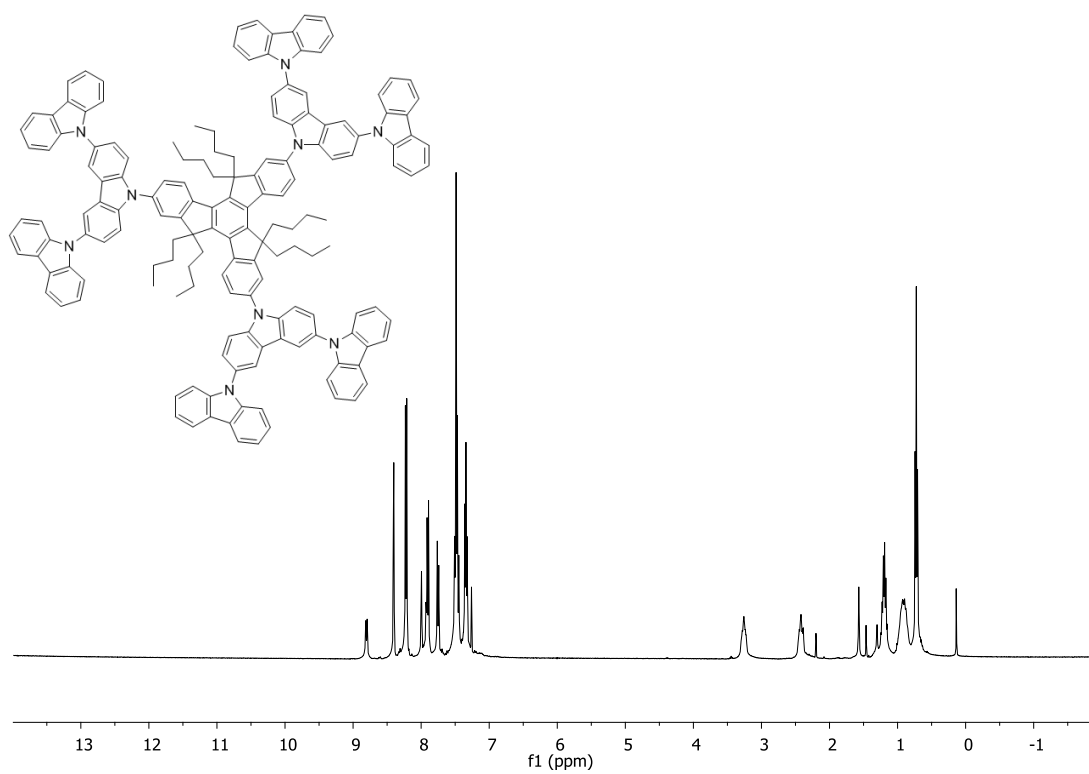


Figure 10 $^1\text{H-NMR}$ spectrum of compound 2

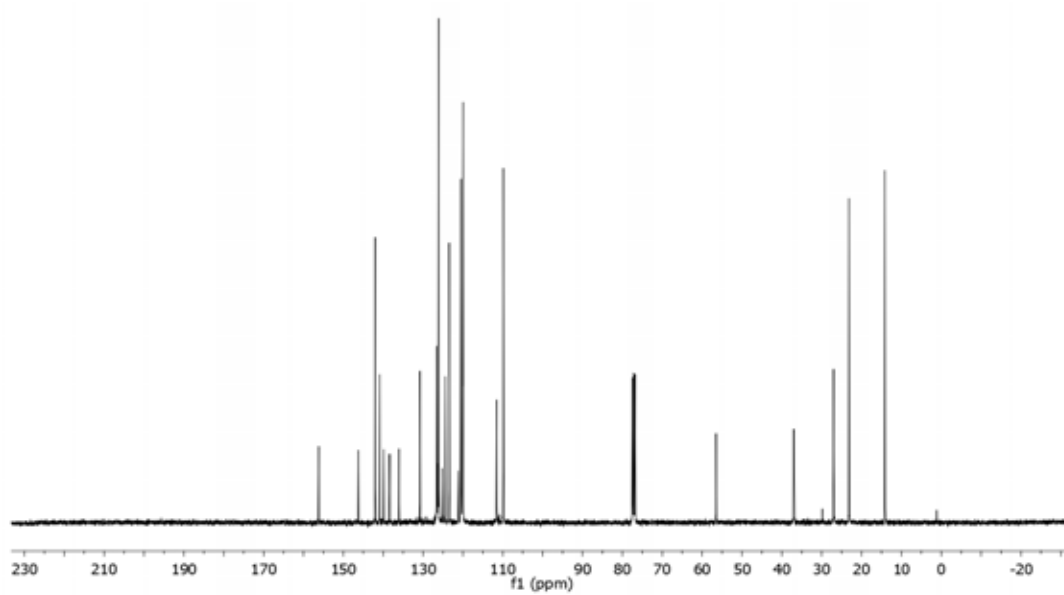


Figure 11 ^{13}C -NMR spectrum of compound 2

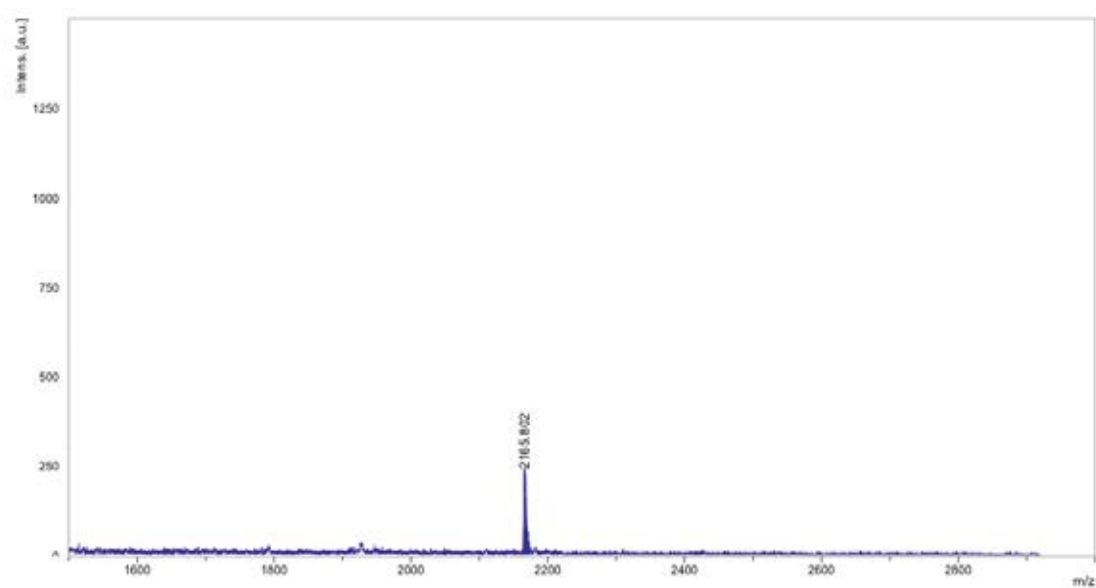


Figure 12 MALDI-TOF spectrum of compound 2

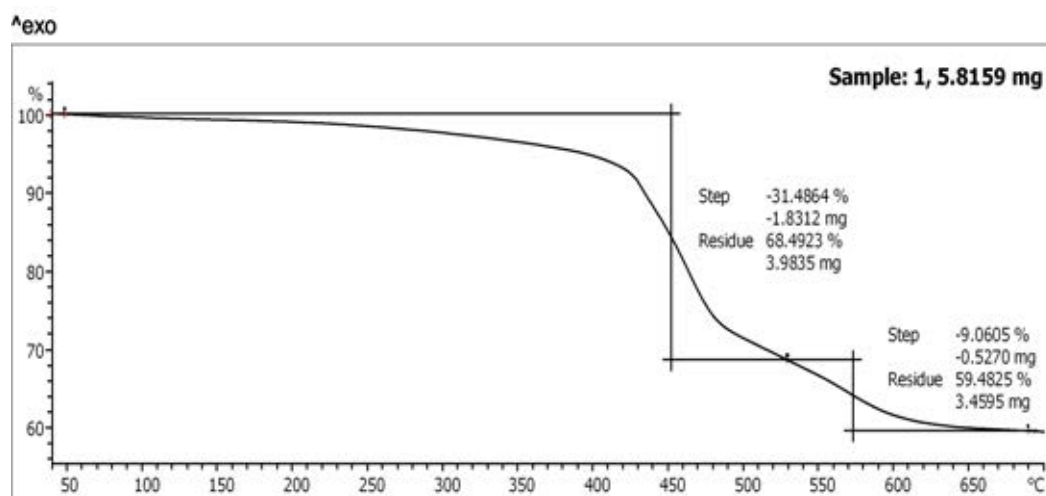


Figure 13 TGA spectrum of compound 1

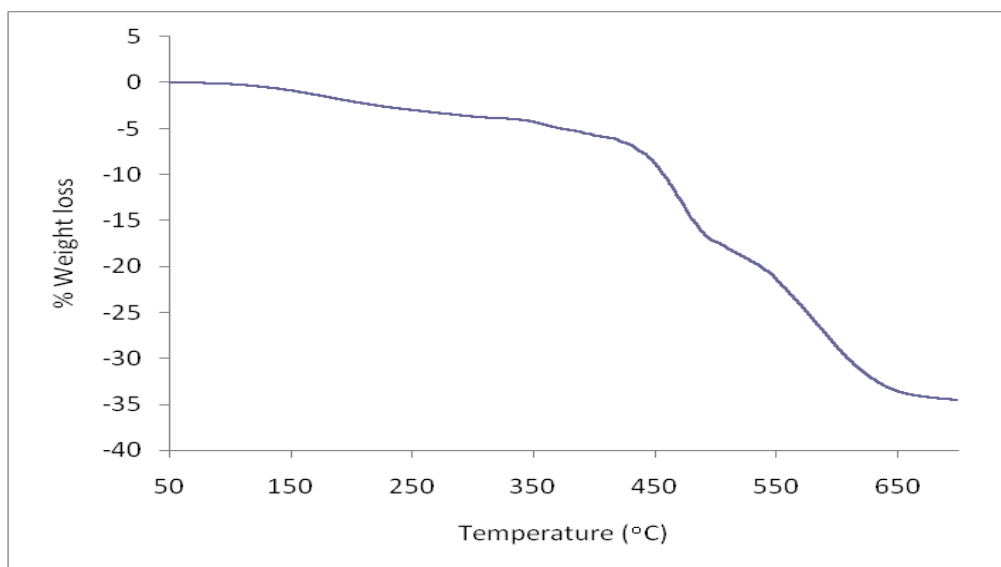


Figure 14 TGA spectrum of compound 2